(4)

AD_____

Molecular Basis of Paralytic Neurotoxin Action on Voltage-Sensitive Sodium Channels

Annual Report

William A. Catterall, Ph.D.
Professor and Chairman
Department of Pharmacology

October 20, 1988

Supported by

U.S. ARMY MEDICAL RESEARCH AND DEVELOPMENT COMMAND
Fort Detrick, Frederick, Maryland 21701-5012

Contract No. DAMD17-84-C-4130

University of Washington
Seattle, Washington 98195

Approved for public release; distribution unlimited

SECURITY CLASSIFICATION OF THIS PAGE

REPORT DOCUMENTATION PAGE

Form Approved
OMB No 0704-0188
Exp Date Jun 30 1986

1a REPORT SECURITY CLASSIFICATION: Unclassified	1b RESTRICTIVE MARKINGS
2a SECURITY CLASSIFICATION AUTHORITY	3 DISTRIBUTION/AVAILABILITY OF REPORT: Approved for public release; distribution unlimited
2b. DECLASSIFICATION/DOWNGRADING SCHEDULE	
4 PERFORMING ORGANIZATION REPORT NUMBER(S)	5. MONITORING ORGANIZATION REPORT NUMBER(S)
6a. NAME OF PERFORMING ORGANIZATION: University of Washington; 6b. OFFICE SYMBOL (If applicable)	7a. NAME OF MONITORING ORGANIZATION
6c. ADDRESS (City, State, and ZIP Code): Department of Pharmacology, Seattle, Washington 98195	7b ADDRESS (City, State, and ZIP Code)
8a. NAME OF FUNDING/SPONSORING ORGANIZATION: U.S. Army Medical Research & Development Command; 8b. OFFICE SYMBOL (If applicable)	9. PROCUREMENT INSTRUMENT IDENTIFICATION NUMBER: DAMD17-84-C-4130
8c. ADDRESS (City, State, and ZIP Code): Fort Detrick, Frederick, MD 21701-5012	10. SOURCE OF FUNDING NUMBERS: PROGRAM ELEMENT NO. 61102A; PROJECT NO. 3M161, 102BS12; TASK NO AA; WORK UNIT ACCESSION NO 111

11. TITLE (Include Security Classification)
(U) Molecular Basis of Paralytic Neurotoxin Action on Voltage-Sensitive Sodium Channels

12. PERSONAL AUTHOR(S)
William A. Catterall, Ph.D.

13a. TYPE OF REPORT	13b. TIME COVERED	14 DATE OF REPORT (Year, Month, Day)	15. PAGE COUNT
Annual Report	FROM 9/15/87 TO 9/14/88	1988, October 20	37

16. SUPPLEMENTARY NOTATION

17. COSATI CODES			18. SUBJECT TERMS (Continue on reverse if necessary and identify by block number)
FIELD	GROUP	SUB-GROUP	Ion transport, sodium channels, action potentials, electrical excitability, neurotoxins
06	01		
06	15		

19. ABSTRACT (Continue on reverse if necessary and identify by block number)

In years 1 - 4 of this project, progress was made on several objectives:

A. The sites and mechanisms of action on the sodium channel were examined and further defined for three new classes of neurotoxins: Goniopora toxins, Brevetoxins, and Conotoxins.

B. Monoclonal antibodies with high affinity for the mammalian neuronal sodium channel were developed and methods to screen them for activity at neurotoxin binding sites were established.

C. Site-directed antibodies against defined regions of the amino acid sequence of the sodium channel were prepared and shown to bind at discrete negatively charged subsites on the extracellular surface of the channel that may form part of neurotoxin receptor sites.

20 DISTRIBUTION/AVAILABILITY OF ABSTRACT: ☒ UNCLASSIFIED/UNLIMITED ☐ SAME AS RPT ☐ DTIC USERS	21 ABSTRACT SECURITY CLASSIFICATION	
22a NAME OF RESPONSIBLE INDIVIDUAL: Mrs. Joy Pawlus	22b TELEPHONE (Include Area Code): 301-663-7325	22c OFFICE SYMBOL: SGRD-RMI-S

DD FORM 1473, 84 MAR — 83 APR edition may be used until exhausted. All other editions are obsolete.

SECURITY CLASSIFICATION OF THIS PAGE

TABLE OF CONTENTS

Foreword

In conducting research described in this report, the investigator(s) adhered to the "Guide for the Care and Use of Laboratory Animals," prepared by the Committee on Care and Use of Laboratory Animals of the Institute of Laboratory Animal Resources. National Research Council (DHEW Publication No. (NIH) 86-23, Revised 1985).

RESEARCH REPORT

In the fourth year of this project, we have concentrated on our efforts on identification of sodium channel receptor site for α-scorpion toxins by analysis with sequence-directed antibodies and on determination of the effects of sequence-directed antibodies on sodium channel function.

I. Photolabeling of the Scorpion Toxin Receptor Site on the R_I and R_{II} Sodium Channel Subtypes

INTRODUCTION

At least five different receptor sites for distinct families of neurotoxins have been shown to be present on voltage-sensitive sodium channels (Ritchie and Rogart, 1977; Catterall, 1980, 1988; Couraud et al., 1982; Poli et al., 1986). α-scorpion toxins bind to neurotoxin receptor site 3 on the sodium channel in a voltage-dependent manner (Catterall,1977; Ray et al., 1978) and modify the activity of the channel by slowing its inactivation and producing a change in the voltage-dependence of inactivation (reviewed by Catterall, 1980; Meves et al, 1986; Strichartz et al, 1987). Purified sodium channels have a principal α subunit of 260 kDa, which is expressed in nerve and muscle in association with one or two smaller β subunits (Agnew, 1984; Catterall, 1984, 1986; Barchi, 1988). The purified sodium channel from rat brain is a complex of three polypeptide subunits: α (260 kDa), β1 (36 kDa), and β2 (33 kDa). The β2 subunit is covalently attached to α by disulfide bond(s), whereas the β1 subunit is noncovalently associated (Hartshorne et al, 1982; Hartshorne & Catterall, 1984). The reconstitution of this purified complex in phospholipid vesicles and planar bilayers shows that these proteins can mediate the functional activities of a voltage-sensitive sodium channel (Talvenheimo et al, 1982; Tamkun et al., 1984; Hartshorne et al., 1985), including voltage-dependent binding of α-scorpion toxin (Feller et al., 1985).

Affinity labeling of sodium channels in synaptosomes and neurons in cell culture with a photoreactive azidonitrobenzoyl (ANB) derivative of the principal α-scorpion toxin (toxin V) from *Leiurus quinquestriatus* (LqTx) yields two specifically labeled polypeptides of 260 kDa and 32-35 kDa (Beneski & Catterall, 1980; Darbon et al., 1983; Sharkey et al., 1984; Jover et al., 1988). The larger polypeptide has been identified as the α subunit of the sodium channel by immunoprecipitation with a specific antiserum (Sharkey et al., 1984), while the smaller polypeptide has been proposed to be the β1 subunit. The α subunit of purified and reconstituted sodium channels is also specifically photolabeled by ANB-LqTx (Messner et al., 1986). We have now examined covalent labeling of the sodium channel α subunit with two different photoreactive derivatives of LqTx and determined their specificity for sodium channel subtypes, allosteric modulation by other neurotoxins, and site(s) of incorporation in the α subunit.

EXPERIMENTAL PROCEDURES

Materials. LqTx was purified from the venom of the scorpion *Leiurus quinquestriatus*, radioactively labeled with $Na^{125}I$ and lactoperoxidase, and repurified to give the monoiodo derivative (Catterall, 1977). Batrachotoxin (BTX) was kindly provided by Dr. John Daly (Laboratory of Bioorganic Chemistry, NIDDK, NIH). Antisera directed against defined peptide segments of the R_I and R_{II} sodium channels from rat brain were prepared as described previously (Gordon et al, 1987, 1988) and IgG

fractions were isolated by precipitation with 50% saturated $(NH_4)_2SO_4$. Anti-$SP11_I$ and anti-$SP11_{II}$ antibodies were affinity-purified by adsorbtion to immobilized sodium channels (Wollner and Catterall, 1986). Antibody volumes refer to the amount of purified antibodies isolated from the equivalent volume of original antiserum.

Synaptosomes were isolated from rat brain by differential and density gradient centrifugation as described previously (Tamkun and Catterall, 1981). Purified sodium channels from rat brain (Hartshorne and Catterall, 1984) at concentrations of 300-400 nM in 25 mM Hepes-Tris, pH 7.4, 100 mM Na_2SO_4, 0.4 mM $MgSO_4$, 157 mM N-acetylglucosamine, 4 µM tetrodotoxin (TTX), 1.65% Triton X-100, 0.19% phosphatidylcholine (PC) and 0.12 % phosphatidylethanolamine (PE) were reconstituted in phospholipid vesicles by removing the detergent from the solution with Bio-beads SM-2 (Tamkun et al, 1984; Feller et al, 1985). The channel reconstituted in this way was immediately used for photolabeling studies. The concentration of purified sodium channels was measured by determination of specific binding of [^{3}H]saxitoxin (STX) using a rapid gel filtration assay for solubilized channels (Hartshorne and Catterall, 1984) or filtration through glass fiber filters for reconstituted vesicles (Tamkun et al, 1984).

Determination of binding of ^{125}I-LqTx to sodium channels. Two hundred µl of reconstituted PC/PE vesicles containing purified sodium channels were desalted by rapid gel filtration using 2 ml Sephadex G-50 columns made with disposable 3 ml syringes. Prior to the addition of the sample, the columns were equilibrated in 24 mM Hepes-Tris, pH 7.4, 140 mM choline chloride, 0.4 mM $MgSO_4$ and 4 mg/ml BSA and prespun in a benchtop centrifuge. A rapid filtration binding assay (Tamkun et al, 1984; Feller et al, 1985) was carried out in 200 µl of the same buffer containing 10 µl of the desalted vesicles and 0.5 nM ^{125}I-LqTx. The nonspecific binding was determined in samples containing 400 nM of unlabeled LqTx. In some cases, either 1 µM TTX or 2 µM BTX or both were present as indicated for each experiment.

Synthesis of ANB-^{125}I-LqTx and MAB-^{125}I-LqTx. All manipulations were carried out in the dark or under red light. Twenty µl of 0.2 M triethanolamine HCl, pH 9.0, were added to 200 µl of 100-150 nM ^{125}I-LqTx in 25 mM sodium phosphate, pH 7.4, 50 mM NaCl and 0.4 mg/ml BSA to give a final pH of 8.3. The coupling reaction was initiated by addition of 1.6 ml of a concentrated solution of ANB N-hydroxysuccinimide in dioxane containing 0.75 mol ANB N-hydroxysuccinimide per mol of lysine residues. After 90 min at room temperature, the addition was repeated and the incubation continued for 90 min more. The reaction was stopped and the excess of reagent was destroyed by adding 1M Tris-HCl to a final concentration of 40 mM.

A similar protocol was followed in the synthesis of MAB-LqTx. In this case, 100 µl of the toxin solution were mixed with 50 µl of triethanolamine HCl. Twenty to 25 equivalents of MAB hydrochloride were added from a cold, freshly prepared solution prepared in 90 mM triethanolamine HCl containing 10% (v/v) dioxane and 4 mg/ml MAB hydrochloride. The reaction was stopped in the same way as for the ANB derivative. The solutions obtained in this way were stored at 4°C and used for photoaffinity labeling experiments within 48h.

Photolabeling of sodium channels. A suspension of synaptosomes (0.5 mg protein/ml) in 50 mM Hepes-Tris, pH 7.4, 130 mM choline chloride, 5.5 mM glucose, 0.5 mM $MgCl_2$, 5.4 mM KCl, 1 mg/ml BSA, 1 µM BTX, 1 µM TTX and 2 nM ANB-^{125}I-LqTX or MAB-^{125}I-LqTx, was incubated in the dark at 37°C for 10 min. The solution was irradiated at 0°C for 10 min with a dual Sylvania blacklite blue fluorescent lamp (λ_{max} 356 nm, 15 W per bulb) which was placed 5 cm from the sample. KCl (4 M) was added to give 150 mM final concentration, and the samples were centrifuged in

microfuge at 4°C. The pellets were resuspended and washed with the same buffer without toxins and containing 135 mM KCl instead of choline chloride to enhance dissociation of noncovalently bound LqTx. The final pellets were used immediately for electrophoresis or stored at -80°C for no more than 7 days.

For photolabeling of purified sodium channels, 30 µl of reconstituted, desalted PC/PE vesicles prepared as described above for the LqTx binding assay, were diluted in 100 µl of binding buffer containing 4 nM photoreactive ^{125}I-LqTx. The solution was incubated and irradiated as described above for synaptosomes. Samples were directly used for electrophoretic analysis or for the isolation of the photolabeled peptides as described below. BTX (1 µM) or 1 µM TTX or both were included as indicated. LqTx (400 nM) was added to some samples in order to determine the nonspecific photolabeling.

Solubilization and purification of photolabeled sodium channels. A pellet containing 250 µg of photolabeled synaptosomes was solubilized at 4°C for 15 min with 150 µl of 20 mM Hepes-Tris, pH 7.4, 50 mM NaCl, 3% Triton X-100, 0.3% PC, 10 µM TTX, containing 16 µg/ml phenyl methanesulfonyl fluoride, 1 µM pepstatin A, and 0.5 mM iodoacetamide as protease inhibitors. Insoluble proteins were separated by centrifugation, and the detergent-solubilized samples were used directly for immunoprecipitation experiments.

For purified and reconstituted sodium channels, 1 ml containing 20 to 30 pmol of photolabeled, reconstituted sodium channels was incubated at 4°C for 20 min in 25 mM sodium phosphate, pH 7.5, 100 mM NaCl, 5 mM EDTA, and 1.5% Triton X-100 and protease inhibitors. WGA-Sepharose (250 µl of a 10% [w/v] suspension) was added, and the samples were mixed by rotation at 4°C for 30 min. The pellet was first extensively washed at 4°C with Buffer S (10 mM Tris-HCl, pH 7.4, 150 mM NaCl, 1 mM EDTA, and 0.5% Triton X-100) containing 4 mg/ml BSA and then twice with the same buffer without BSA. The proteins bound to WGA-Sepharose were eluted by washing three times at 0°C for 5 min with 250 µl 0.2 M N-acetylglucosamine in buffer S. This solution was stored at -80°C and used within two weeks for immunoprecipitation and proteolysis experiments.

RESULTS

Photoaffinity labeling of rat brain sodium channels. Two different photoreactive derivatives of LqTx have been synthesized by coupling photoactivable reagents to free amino groups on the polypeptide toxin. Lysine 60 has been shown to be the preferred site of reaction of amino group reagents with LqTx with lys 58 as a secondary site (Darbon et al, 1983b). ANB N-hydroxysuccinimide is expected to give an uncharged amide adduct while MAB hydrochloride is expected to give an imidine adduct which retains the original charge of the lys residue. Irradiation of synaptosomal fractions with long wavelength UV light in the presence of specifically bound ^{125}I-ANB-LqTx results in the specific photolabeling of two proteins of 270 kDa and 37 kDa when analyzed by SDS-PAGE as shown in Fig. 1A (lane 2). This labeling is blocked by incubation with excess unlabeled LqTx (Fig. 1A, lane 4). In previous work, the 270 kDa protein has been identified as the α subunit of the sodium channel by immunoprecipitation with antibodies, whereas the 37 kDa protein has been identified as the β1 subunit based on its apparent molecular weight (Beneski and Catterall, 1980; Sharkey et al, 1984). In contrast, [^{125}I]MAB-LqTx specifically photolabels only the 270 kDa band in synaptosomes (Fig. 1B, lanes 2 and 4). Reduction of the 300 kDa disulfide-linked αβ2 complex did not yield additional photolabeled bands of low molecular weight

(Fig. 1 A and B, compare lanes 1 and 2) indicating that β2 subunits are not labeled. The introduction of a large excess of coupled MAB groups on the toxin does not produce any additional specifically photolabeled protein bands (Fig. 1C). These results indicate that the two photoreactive derivatives of LqTx label the sodium channel complex in synaptosomes differently.

Both ANB and MAB derivatives photolabeled only the α subunit in preparations of purified sodium channels reconstituted in phospholipid vesicles (Fig. 2, lanes 1 and 3). Incorporation of the photolabel into the α subunit was completely blocked by incubation with unlabeled LqTx (Fig. 2, lanes 2 and 4). The intense photolabeled protein band of about 65 kDa is BSA which was used as a scavenger to reduce the nonspecific labeling in the photoreaction. No protein band of 37 kDa was photolabeled in this purified preparation, even though β1 subunits are present in equal stoichiometry to α subunits (Hartshorne and Catterall, 1984). Evidently, the receptor site for α-scorpion toxins is located on the α subunit of the sodium channel. LqTx bound at this site can, under some conditions, label the nearby β1 subunit.

Photolabeling of the R_I and R_{II} sodium channel subtypes from rat brain. Anti-SP11$_I$ and anti-SP11$_{II}$, specific antibodies against R_I and R_{II} rat brain sodium channel subtypes respectively (Gordon et al, 1987), are able to immunoprecipitate photolabeled sodium channel α subunits from synaptosomes (Fig. 3, lanes 1 and 3). No photolabeled protein bands are immunoprecipitated from samples labeled under conditions of nonspecific binding in the presence of excess unlabeled LqTx (Fig. 3, lanes 2 and 4). These results show that the α subunits of both the R_I and R_{II} sodium channel subtypes have high affinity binding sites for LqTx.

Purified preparations of sodium channels from rat brain are approximately 75% R_{II} and 25% R_I (Gordon et al, 1987). Photolabeled α subunits are immunoprecipitated by anti-SP11$_I$ and anti-SP11$_{II}$ antibodies (Fig. 3B, lanes 1 and 3). No photolabeled protein bands are immunoprecipitated when the photolabeling reaction is carried out in the presence of excess unlabeled LqTx (Fig. 3, lanes 2 and 4). Since the immunoprecipitation of purified and reconstituted sodium channels was carried out with saturating quantities of the two antibodies, these results can be compared quantitatively with the relative amount of R_I and R_{II} present in the purified preparations. As expected, approximately 3-fold more radioactive toxin is incorporated into the R_{II} channel consistent with its 3-fold higher concentation in the purified preparation.

Both R_I and R_{II} sodium channel α subunits are expressed as disulfide-linked complexes with β2 subunits (Gordon et al, 1988). Affinity purified anti-β2 antibodies immunoprecipitated a 300 kDa band in the unreduced photolabeled sodium channel (Fig. 3B, lane 5). When disulfide bonds are reduced, the photolabeled α subunits are no longer immunoprecipitated by anti-β2 antibodies (Fig. 3B, lane 6), demonstrating that β2 subunit is covalently attached to the photolabeled α subunit in purified sodium channels of both subtypes.

Allosteric modulation of LqTx binding and photolabeling of purified and reconstituted sodium channels. It has previously been shown that reconstitution of purified sodium channels in vesicles of defined phospholipid composition restores the specific binding of LqTx with the high affinity and voltage-dependence characteristic of native sodium channels (Tamkun et al, 1984; Feller et al, 1985). In intact membranes, binding of LqTx is also modulated by neurotoxins acting at sites 1 and 2 on the sodium channel (Ray et al, 1978; Catterall et al, 1979). This allosteric modulation was not systematically examined in previous reconstitution studies. The results of Fig. 4A show that both TTX and BTX enhanced the binding of ^{125}I-LqTx, as expected from studies of

toxin binding to sodium channels in intact mambranes. Their effects were additive when both BTX and TTX were present. Thus, the interactions among neurotoxins bound at different receptor sites in native sodium channels are recovered in purified and reconstituted sodium channels.

Modulation of photoaffinity labeling by BTX and TTX was examined for both ANB and MAB derivatives of LqTx. As illustrated in Fig.5A, both BTX (lane 2) and TTX (lane 3) increase the photoaffinity labeling of α subunits by MAB-^{125}I-LqTx compared to the control sample (lane 1). Their effects are additive (Fig. 5A, lane 4). This pattern of photolabeling by MAB-LqTx follows closely the changes in binding of native LqTx as illustrated quantitatively in Fig. 4B (hatched bars). In contrast, these toxins did not produce significant effects on the photolabeling of the α-subunit by ANB-LqTx (Fig. 5B). These results differ sharply from the pattern of binding observed for native LqTx (Fig. 4B, open bars). The different results observed with ANB and MAB derivatives of LqTx suggest that the loss of the positive charge of the lysine residues to which the photoreactive groups are attached alters the allosteric interactions between LqTx binding and binding of BTX and TTX.

Proteolytic fragments of the photolabeled α subunit. In order to test whether the labeling within the photolabeled α subunit is distributed along the molecule or concentrated in a specific domain, the α subunit was isolated and subjected to proteolysis with *S. aureus* protease V8 or chymotrypsin. Both enzymes produce fragments of 60-70 kDa containing most of the covalently bound LqTx of α subunits photolabeled by ANB-LqTx (Fig. 6A) or MAB-LqTx (Fig. 6B). This suggests that both reagents labeled the same region within the structure of the α subunit despite the differences in their binding interactions with the sodium channel..

DISCUSSION

Location of the receptor site for α-scorpion toxins. Previous experiments on photoaffinity labeling of the receptor site for α-scorpion toxins with ANB-LqTx resulted in covalent labeling of polypeptides of 260 kDa and 32-37 kDa in synaptosomes (Beneski and Catterall, 1980; Sharkey et al, 1984; Jover et al, 1988; Fig. 1). Since both 260 kDa and 32-37 kDa polypeptides were substantially labeled, these results did not clearly define which one actually contained the toxin receptor site. Our present results indicate that the 260 kDa α subunit of the sodium channel is the target of α-scorpion toxins since it is the only protein specifically labeled by both ANB and MAB derivatives of LqTx. In purified and reconstituted preparations of native sodium channels, both photoactivable derivatives of LqTx label the α subunit exclusively. In synaptosomes, ANB-LqTx labels polypeptides of 260 kDa and 37 kDa, while MAB-LqTx labels only the α subunit, even when heavily substituted toxin preparations are used. Since purified and reconstituted sodium channels bind LqTx with similar affinity, voltage dependence, and allosteric interactions as native sodium channels, it is likely that the site of covalent labeling in purified sodium channels represents the normal site of interaction in native sodium channels and, therefore, that this site is located on the α subunit.

High affinity binding of LqTx to sodium channel subtypes. Two different sodium channel α subunit subtypes, R_I and R_{II}, are expressed in the adult rat brain (Noda et al, 1986; Gordon et al, 1987). These two α subunits are 87% identical in amino acid sequence (Noda et al, 1986), but their comparative functional properties are unknown because the R_I subtype is poorly expressed from cloned DNA. We show here that α subunits of both the R_I and R_{II} sodium channel subtypes are labeled to an approximately equivalent extent by photoreactive derivatives of LqTx and are expressed in disulfide

linkage with β2 subunits. Since high affinity binding of LqTx is required for efficient photoaffinity labeling, we conclude that these two sodium channel subtypes both have high affinity for LqTx.

Allosteric modulation of the binding of LqTx to purified and reconstituted sodium channels. In previous studies of purified and reconstituted sodium channels (Tamkun et al, 1984; Feller et al, 1985), the modulation of the binding of ^{125}I-LqTx by neurotoxins which interact with receptor sites 1 and 2 was not reproducibly observed, in contrast to previous work with native synaptosomal sodium channels (Ray et al, 1978; Catterall et al, 1979; Tamkun and Catterall, 1981). In our present experiments using a reconstitution protocol modified as described by Messner et al (1986), BTX and TTX caused additive increases in the binding of LqTx in close correspondence to results expected from studies in synaptosomes. Thus, reconstituted sodium channels retain the allosteric interactions characteristic of native sodium channels. The effect of TTX deserves mention since its effects on LqTx binding in synaptosomes were previously interpreted as a consequence of block of the loss of synaptosomal K^+ and the resulting synaptosomal depolarization due to LqTx (Ray et al, 1978). This cannot be the explanation for our results in reconstituted vesicles since exit of intravesicular Na^+ ions will serve to hyperpolarize the vesicles and increase LqTx binding. The effect of TTX to increase LqTx binding most likely represents an allosteric effect of toxin binding rather than an indirect effect of blocking ion conductance by the sodium channel.

Differential binding and photolabeling of ANB-LqTx and MAB-LqTx. Two differences in the mechanisms of action of ANB-LqTx and MAB-LqTx were observed in these studies. Binding of MAB-LqTx is modulated by neurotoxins like the binding of native LqTx, while binding of ANB-LqTx is not; and MAB-LqTx labels only the α subunit of the sodium channel in synaptosomes, while ANB-LqTx specifically labels 260 kDa and 37 kDa polypeptides in synaptosomes. The different results obtained with these two different derivatives of LqTx may be the consequence of the difference in charge between the reaction products formed by ANB-LqTx and MAB-LqTx. While the positive charge of the derivatized amino groups of the toxin is eliminated by formation of an amide bond in ANB-LqTx, this charge is conserved at physiological pH as an imidine in MAB-Lqtx. The differences in allosteric modulation and in photolabeling patterns in synaptosomes suggest that the change in charge of the toxin derivative modifies some aspects of the conformation of its complex with the sodium channel, thereby altering its allosteric interactions within the α subunit and allowing photoreaction with the nearby β1 subunit under some conditions.

Photolabeling of a discrete region of the α-subunit by ANB-LqTx and MAB-LqTx. Although the ANB and MAB derivatives of LqTx differ in their allosteric interactions with other sodium channel ligands and in labeling of different sodium channel subunits, both MAB- and ANB-LqTx seem to label the same region within α subunit. Proteolytic digestion of the α subunit photolabeled with either derivative, under conditions where LqTx itself is not cleaved, yields a single major proteolytic product of 60 to 70 kDa with both *S. aureus* V8 protease and chymotrypsin. These results indicate that both derivatives are attached in a similar region of the sodium channel α subunit and that the incorporated photolabel is not broadly distributed throughout the protein. Since the labeling of the α subunit seems to be restricted to a discrete region of its structure, this photoaffinity labeling approach may be valuable in localizing neurotoxin receptor site 3 within the amino acid sequence of the α subunit and, in this way, establishing the structure-function relationships in an extracellular region of sodium channels in which bound neurotoxins can modify channel inactivation.

II. Site of Covalent Labeling of the Scorpion Toxin Receptor Site on the Sodium Channel α Subunit

INTRODUCTION

Since photoreactive LqTx derivatives label a discrete domain within the sodium channel α subunit subunit; determination of the site of covalent labeling will identify a region of the sodium channel located in or near the LqTx receptor site. We have developed a novel approach using sited-directed antibodies to identify the site of covalent attachment of LqTx.

EXPERIMENTAL PROCEDURES

Photoaffinity labeling of sodium channel. Purified and reconstituted sodium channels (200 µl of 25 nM) were desalted by rapid gel filtration on 2 ml Sephadex G-50 columns equilibrated with 10 mM Hepes-Tris, pH 7.4, isotonic sucrose and 4 mg/ml BSA (Darbon et al, 1983). The desalted vesicles were diluted with one volume of the same buffer containing 20 nM ANB-^{125}I-LqTx, 2 µM batrachotoxin, and 1 µM TTX. The solution was incubated at 37°C for 10 min and irradiated at 0°C for 10 min using a dual Sylvania blacklite blue fluorescent lamp (λ_{max} 356 nm, 15 w per bulb) which was placed at 5 cm from the sample. One µM LqTx was present in some samples in order to determine nonspecific photolabeling.

Isolation of photolabeled sodium channels. One ml of photolabeled reconstituted sodium channel was solubilized by incubation at 4°C for 20 min in 25 mM sodium phosphate, pH 7.5, 100 mM NaCl, 5 mM EDTA, and 1.5% Triton X-100 containing 16 µg/ml PMSF, 1 µM pepstatin A, and 0.5 mM iodoacetamide as protease inhibitors. 250 µl of 10% (w/v) WGA-Sepharose were then added and the sample was mixed by rotation at 4°C for 30 min. The pellet was first extensively washed at 4°C with Buffer S (10 mM Tris-HCl, pH 7.4, 150 mM NaCl, 1 mM EDTA) containing 0.5% Triton X-100 and 4 mg/ml BSA, and then twice with the same solution without BSA. The proteins bound to WGA-Sepharose were eluted by washing three times for 5 min each at 0°C with 250 µl of 0.2 M N-acetylglucosamine, 0.1% Triton X-100 in Buffer S. This solution was stored at -80°C and used within two weeks for proteolysis experiments.

Immunoprecipitation of photolabeled sodium channel. Affinity-purified antibodies were incubated with photolabeled sodium channel preparations, or fragments prepared from them, overnight at 0°C in Buffer S containing 1% Triton X-100 and 1 mg/ml BSA. One mg of Protein A-Sepharose per µl of serum was added from a 10% suspension prepared in the same solution. The samples were mixed by rotation at 4°C for 30 min. Supernatants were removed and the pellets were washed twice with 10 volumes of Buffer S containing 4 mg/ml BSA and once with 5 volumes of the same solution without BSA. The proteins were finally solubilized from the pellet with NaDodSO$_4$-PAGE loading solution by incubation at 100°C for 2 min, and the samples were analyzed by NaDodSO$_4$-PAGE and autoradiography.

Electrophoresis methods. Three gel electrophoresis systems have been used. System A was a standard NaDodSO$_4$-PAGE method with 9% polyacrylamide gels (Maizel, 1971). System B consisted of a 5-20% linear gradient polyacrylamide gel prepared with a 30:0.8 ratio of acrylamide to N,N'-methylene-bis-acrylamide (Maizel, 1971). System C was a modification of the method of Kyte and Rodriguez (Kyte &

Rodriguez, 1983) with a 3.5% polyacrylamide stacking gel and a 10% polyacrylamide separation gel. A good resolution of peptides ranging from 2 to 45 kDa is obtained with ystem C.

RESULTS AND DISCUSSION

Isolation of a 48 kDa glycoprotein fragment of the α subunit containing covalently attached LqTx. Purified rat brain sodium channels were reconstituted in PC/PE vesicles under conditions (Feller et al, 1985) which give efficient recovery of high affinity binding of the α-scorpion toxin (toxin V, Rochat et al, 1979) from *Leiurus quinquestriatus* (LqTx). LqTx binding to sodium channels reconstituted in vesicles under these conditions is modulated by membrane potential and by allosteric interactions with neurotoxins binding at sites 1 and 2 as for sodium channels in intact membranes (Messner et al, 1986; Tejedor & Catterall, 1988). The α subunits of the sodium channels in these reconstituted vesicles were specifically labeled with a photoreactive derivative of LqTx (ANB-^{125}I-LqTx) (Fig. 7A, lanes 1 and 2) and isolated by affinity chromatography on WGA-Sepharose. This one-step purification yields a single labeled protein of approximately 300 kDa (Fig. 7B, lane 1) that was identified as the disulfide-linked complex of the α and β2 subunits of the sodium channel by immunoprecipitation with specific anti-α and anti-β2 antibodies (Messner et al, 1986; Tejedor & Catterall, 1988).

In preliminary experiments, proteases were screened to find experimental conditions under which the α subunit could be cleaved while the LqTx label remained intact. Chymotrypsin, *S. aureus* protease V8, elastase, TPCK-trypsin, and thermolysin all cleave the α subunit without cleaving LqTx when disulfide bonds are not reduced, probably because LqTx has a compact, highly disulfide-bonded structure (Rochat et al, 1979; Fonteciila-Camps et al, 1982). Proteolysis of the photolabeled αβ2 complex under nonreducing conditions with these four proteases yields a single major labeled fragment of 55 to 72 kDa in each case (Fig. 7B). Since these proteases cleave at different amino acid residues, these results suggest that most of the covalently attached LqTx is located within a structurally compact, relatively protease-resistant domain of approximately 55 to 72 kDa within the α subunit. This region is rich in N-linked carbohydrate chains since digestion of the 72 kDa photolabeled fragment produced by protease V8 with neuraminidase yields a desialylated polypeptide of 55 kDa (Figure 7C). Since the molecular mass of LqTx is 6.7 kDa, these results imply that the molecular mass of the desialylated glycoprotein produced by treatment with protease V8 and neuraminidase is approximately 48 kDa.

Covalent attachment of α-scorpion toxin to a site in domain I of the α subunit. Since photoactivable derivatives of LqTx covalently label only 2 to 5% of the α subunits to which they are specifically bound (R. Sharkey and W.A. Catterall, unpublished results), isolation of a sufficient quantity of labeled peptide fragments for determination of their amino acid sequence is difficult. Therefore, we have used a battery of antibodies directed against synthetic peptides whose amino acid sequences correspond to defined segments (Fig. 8A) of the α subunit of rat brain sodium channel R_{II} (Noda et al, 1986) to identify the site of covalent attachment. Immunoprecipitation with antibodies that recognize α subunit segments ranging from the N-terminal to the C-terminal (Fig. 8A) showed that only anti-$SP_{317-335}$ (not shown) and anti-$SP_{382-400}$ (Fig. 9, lane 2), which recognize a proposed extracellular segment in domain *I*, immunoprecipitated the photolabeled 72 kDa glycopeptide produced by proteolysis with V8 protease. Immunoprecipitation by both antibodies was blocked by prior incubation with the corresponding peptide, demonstrating its specificity (Fig. 9, lane 3). This experiment

approximately localizes the labeled region within the first of the four homologous domains of the α subunit (Noda et al, 1986), since antibodies directed against SP_{31-47}, located in the N-terminal proposed intracellular segment, and $SP_{427-445}$, located immediately on the C-terminal side of the transmembrane segment IS6, did not immunoprecipitate the photolabeled 72 kDa V8 glycopeptide fragment.

In order to locate the photolabeled region more precisely, we carried out partial proteolytic digestions followed by immunoprecipitation with anti-$SP_{317-335}$, anti-$SP_{382-400}$, or anti-$SP_{427-445}$, which bind within the C-terminal region of domain I. As shown in Fig. 10A, all three antibodies are able to recognize 105 kDa and 82 kDa photolabeled fragments produced by protease V8, but anti-$SP_{427-445}$ failed to recognize the final 72 kDa glycopeptide in agreement with the results of Fig. 9. This experiment shows that the final cleavage by V8 protease, which is highly specific for cleavage at glu or asp residues, eliminates the immunoreactivity of the photolabeled fragment toward anti-$SP_{427-445}$. There are no glu or asp residues between glu_{429}, which is in $SP_{427-445}$, and glu_{387}, which must remain in the photolabeled fragment since it is recognized by anti-$SP_{382-400}$ (Fig. 8B). Therefore, this final cleavage by V8 protease must take place at one of the six glu residues within peptide $SP_{427-445}$, and the C-terminal of the 48 kDa glycopeptide segment must be located between glu_{429} and glu_{443}. The size of this fragment (48 kDa) indicates that it may contain as many as 420 amino acids, depending upon the contribution of the desialylated core of the N-linked carbohydrate chains to its apparent size. Thus, this fragment contains most or all of homologous domain I, which includes residues 125 to 427.

The experiment illustrated in Fig. 10B eliminates an additional segment at the C-terminal end of domain I. The purified photolabeled αβ2 complex was desialylated by treatment with neuraminidase and cleaved with 1, 10, or 100 μg/ml of TPCK-trypsin. The highest concentration of trypsin produced two photolabeled cleavage products of 46 kDa and 37 kDa, corresponding to desialylated α subunit glycopeptide masses of 39 kDa and 30 kDa. Anti-$SP_{317-335}$, anti-$SP_{382-400}$, and anti-$SP_{427-445}$ all precipitated the 39 kDa desialoglycopeptide, but neither anti-$SP_{382-400}$ nor anti-$SP_{427-445}$ immunoprecipitated the 30 kDa desialoglycopeptide. Since TPCK-trypsin is highly specific for cleavage at lys and arg residues, the last cleavage which removes the immunoreactivity toward anti-$SP_{382-400}$ must take place at lys_{355}, arg_{358}, or arg_{378}, the only lys or arg residues between $SP_{317-335}$ and $SP_{382-400}$ (Fig. 8B). The size of this small fragment (30 kDa) indicates that it may contain up to 260 amino acids, depending upon the contribution of the desialylated core of the N-linked carbohydrate chains to its apparent mass. Therefore, the C-terminal of this 30 kDa fragment is located between residues 355 and 378, and its N-terminal may extend as far as residue 95. This region of domain I contains transmembrane segments S1, S2, S3, S4, S5, the hydrophilic segments connecting them, and approximately half of the proposed extracellular segment between transmembrane segments S5 and S6.

Identification of a 14 kDa peptide fragment of the α subunit that is covalently labeled by LqTx. In order to generate smaller fragments of the α subunit which contain covalently attached LqTx, we digested labeled α subunits with trypsin to produce fragments of approximately 70 kDa (Fig. 7B, lane 5) and then cleaved these polypeptides at methionine residues with CNBr. This approach permitted us to work with denatured and reduced sodium channel preparations without cleaving LqTx, since there are no met residues in LqTx V (Rochat et al, 1979). After CNBr digestion, most of the radioactivity is recovered in a peptide whose size is similar to LqTx. Lower intensity photolabeled protein bands of 50 kDa and 21 kDa are also observed. These larger peptides are specifically immunoprecipitated by anti-$SP_{317-335}$ and anti-$SP_{382-400}$ (Fig. 11A), but not by anti-$SP_{427-445}$ (not shown). When the same peptide fragments were prepared

from photolabeled α subunits that had been incubated with neuraminidase, the 50 kDa fragment was reduced to 43 kDa while the size of the 21 kDa photolabeled fragment was unaffected (Fig. 11B). The labeled peptide band of 21 kDa corresponds to a 14 kDa sodium channel fragment without the covalently attached LqTx. Since the apparent size of this fragment is not affected by neuraminidase treatment, it is unlikely to contain complex N-linked carbohydrate chains. If it is unglycosylated, its length would be approximately 120 amino acids.

In contrast to the 50 and 21 kDa CNBr digestion products, none of the available antibodies specifically recognized the small fragment similar in size to free LqTx. This small fragment might represent free LqTx released from covalent attachment to the α subunit by the CNBr treatment or LqTx covalently attached to a fragment of less than 20 amino acids that is not recognized by any of the available antibodies.

Location of the site of covalent attachment of LqTx. Our results sharply restrict the possible locations of the site of covalent attachment of LqTx, but do not yet precisely determine the amino acid residues involved. Analysis of cleavage products from limited proteolytic digestions with V8 protease restrict the C-terminal end of the labeled peptide to residue 427 (Figure 10A). Similar experiments with trypsin restrict it further to residue 379 (Figure 10B). These results place the C-terminal limit for the location of the site of covalent attachment of LqTx at arg_{379}. The major site of LqTx attachment must be located toward the N-terminal from this site since most of the LqTx label is immunoprecipitated in a single fragment (Fig. 7) that is recognized by our antibodies (Figs. 9 and 10).

The N-terminal limit for the location of the site of covalent attachment of LqTx is established by analysis of the properties of the CNBr peptide of 14 kDa with covalently attached LqTx. Inspection of the amino acid sequence of the α subunit (Fig. 8B) shows that the C-terminal of this CNBr peptide must be at met_{402} or met_{426}, since these are the only two met residues between peptides $SP_{382-400}$ and $SP_{427-445}$ where the N-terminal of this fragment must be located (Fig. 11). Considering the size of this peptide, its N-terminal could conceivably be located at met_{313}, met_{270}, or met_{252}. The minimum mass of the polypeptide portion of this fragment is 10.2 kDa, the mass contributed by amino acid residues 313 to 402.

Consideration of the contribution of N-linked glycosylation to the size of the peptide fragments we have characterized allows a clear choice among these three possible N-termini. The V8 fragment containing most of domain I is reduced in apparent size from 72 kDa to 55 kDa by treatment with neuraminidase (Fig. 7C). Approximately half of the mass of N-linked carbohydrate of the total α subunit is accounted for by sialic acid, as measured by direct chemical analysis or by treatment with glycosidases and $NaDodSO_4$-PAGE analysis (Grishin et al, 1984; Elmer et al, 1985; Schmidt & Catterall, 1987). Thus, as much as 34 kDa of N-linked carbohydrate may be attached to glycosylation sites in domain I. There are 7 possible sites of attachment: asn_{212}, asn_{285}, asn_{291}, asn_{297}, asn_{303}, asn_{308}, and asn_{340}. Five of these lie between met_{270} and met_{313}. Since the typical mass of an N-linked carbohydrate chain is 3 to 4 kDa, it is likely that most, if not all, of these possible glycosylation sites contain N-linked carbohydrate chains. If the 14 kDa fragment to which LqTx is covalently attached included the peptide segment from residues 270 to 313 which contains five sites of glycosylation it would have a peptide mass of 15 kDa plus 17 to 34 kDa of N-linked carbohydrate. Since this fragment is only 14 kDa and contains no sialic acid, we conclude that its N-terminal end is likely to be located at met_{313}. With this N-terminal, the size of the 14 kDa fragment can be accounted for in either of two ways. If the C-terminal is at met_{426}, the protein mass of the predicted polypeptide is 13 kDa in close

agreement with the experimental observations without consideration of possible glycosylation. If the C-terminal is at met_{402}, the protein mass of 10.2 kDa plus the expected size of an N-linked carbohydrate chain at asn_{340} would give approximately 14 kDa. In either case, the C-terminal limit for the location of the site of covalent attachment of LqTx would be at met_{313}.

LqTx derivatives prepared by reaction at amino groups consist of a mixture of isomers substituted on lys residues 58 or 60 (Darbon et al, 1983), which are located on the periphery of the array of highly conserved amino acid residues that is thought to define the active site for binding to the sodium channel (Rochat et al, 1979; Fontecilla-Camps et al, 1982; El Ayeb et al, 1986). The corresponding lys residues of some α-scorpion toxins are essential for toxicity (Rochat et al, 1979). We expect, therefore, that the site of covalent attachment of LqTx to the sodium channel is close to the active site for toxin binding. Neither anti-$SP_{317-335}$ nor anti-$SP_{382-400}$ block LqTx binding (unpublished results), indicating that neither of these peptide segments is an essential part of the toxin receptor site on the α subunit. Therefore, it seems most likely that the site of covalent attachment of LqTx derivatives and at least a portion of the site of toxin binding are located between amino acid residues 335 and 378. Since high affinity LqTx binding activity requires the native conformation of the sodium channel (Tamkun et al, 1984; Feller et al, 1985), it is likely that multiple polypeptide segments from different regions of the α subunit contribute to formation of the active receptor site in its native conformation. Further analysis of the interactions between LqTx and sodium channel segments in the extracellular region of domain I using synthetic peptides and anti-peptide antibodies may provide a more complete understanding of the multiple polypeptide segments of the sodium channel which form the receptor site for LqTx.

Transmembrane topology of the α subunit. The α-scorpion toxins modify sodium channel properties from the extracellular surface of the channel (Catterall, 1980; Meves et al, 1986; Strichartz et al, 1987). Therefore, our results provide direct evidence that at least a portion of the segment of the α subunit located between amino acid residues 335 and 378 is extracellular as illustrated in Figure 8. We have previously shown that the long hydrophilic segment between domains I and II contains at least four sites of *in vivo* phosphorylation by cAMP-dependent protein kinase (Rossie et al, 1987), defining this segment as intracellular. Considered together, these two lines of evidence confirm the presence of at least one transmembrane segment, IS6, between the intracellular phosphorylation sites and the site of covalent attachment of LqTx. These results are also compatible with the location of three transmembrane segments between these two sites as suggested in two alternative models for the transmembrane folding of the α subunit (Guy & Seetharamulu, 1986; Greenblatt et al, 1985). Additional direct experimental information is required to define the transmembrane folding pattern within the homologous domains of the sodium channel α subunit more completely.

III. Identification of an Intracellular Peptide Segment Involved in Sodium Channel Inactivation

Antibodies against conserved segments. Antibodies against a peptide (SP19) corresponding to a highly conserved, predicted intracellular region of the sodium channel α subunit bind rat brain sodium channels with a similar affinity as the peptide antigen, indicating that the corresponding segment of the α subunit is fully accessible in the intact channel structure. These antibodies recognize sodium channel α subunits from rat or eel brain, rat skeletal muscle, rat heart, eel electroplax and locust nervous system. Alpha subunits from all these tissues except rat skeletal muscle are substrates for phosphorylation by cAMP-dependent protein kinase. Disulfide-linkage of α and β2

subunits was observed for both the R_I and R_{II} subtypes of rat brain sodium channels and for sodium channels from eel brain, but not for sodium channels from rat heart, eel electroplax, or locust nerve cord. Treatment with neuraminidase reduced the apparent M_r of sodium channel α subunits from rat and eel brain and eel electroplax by 22,000 to 58,000, those from heart by 8,000, and those from locust nerve cord by less than 4,000. Our results provide the first identification of sodium channel α subunits from rat heart and locust brain and nerve cord and show that sodium channel α subunits are expressed with different subunit associations and posttranslational modifications in different excitable tissues.

Studies with site-directed antibodies which specifically recognize the R_I and R_{II} sodium channel subtypes show that they are the primary sodium channel subtypes expressed in spinal cord and brain, respectively, but are not measurably expressed in skeletal muscle, heart, and several sites in the peripheral nervous system (Gordon et al, 1987). In order to study the conserved features of sodium channels in a wide range of excitable tissues, we have developed site-directed antibodies against highly conserved segments of the α subunits.

Modulation of inactivation by antibodies. Voltage-sensitive sodium channels mediate the rapid increase in Na^+ permeability during the rising phase of the action potential in many excitable cells (Hille, 1984). Their ion conductance is regulated on the millisecond time scale by two experimentally separable processes: voltage dependent activation, which controls the rate and voltage dependence of the Na^+ conductance increase upon membrane depolarization, and inactivation, which mediates the Na^+ conductance decrease during a maintained depolarization (Hille, 1984). Messenger RNA encoding the α subunit is sufficient to direct the synthesis of functional Na^+ channels in *Xenopus* oocytes (Goldin et al, 1986; Noda et al, 1986b), although their inactivation is slower than native Na^+ channels (Auld et al, 1988). The primary structures of Na^+ channel α subunits from rat brain and eel electroplax have been inferred from the nucleotide sequence of cDNA clones (Noda et al, 1984; Noda et al, 1986). Na^+ channel α subunits consist of four homologous transmembrane domains that have approximately 50% amino acid sequence identity (Fig. 12A) (Noda et al, 1984; Noda et al, 1986). These are connected by hydrophilic segments that are predicted to be intracellularly oriented (Fig. 12A). Electrophysiological studies have shown that intracellular application of proteases and amino acid-specific reagents causes removal of Na^+ channel inactivation (Armstrong et al, 1973; Eaton et al, 1978; Oxford et al, 1978; Patlak & Horn, 1982). These results indicate that regions of the Na^+ channel structure that are required for inactivation are located on the intracellular surface of the channel protein and are accessible to macromolecular reagents.

To identify functionally important regions on the intracellular surface of the Na^+ channel, we studied the functional effects of antibodies (Gordon et al, 1987; Gordon et al, in press; Merrick & Catterall, unpublished results) against synthetic peptides (SP1, SP11, SP19, and SP20) with amino acid sequences that correspond to both conserved and variable sequences (Table 1) of the intracellular segments between the four homologous domains of Type II rat brain Na^+ channel (R_{II}, Noda et al, 1984; Noda et al, 1986) (Fig. 1A). These antibodies recognize the Na^+ channel purified from rat brain in native form, and their affinity for the native protein is comparable to their affinity for the peptide used as antigen (Gordon et al, 1987; Gordon et al, in press; Merrick & Catterall, unpublished results). The functional effects of these antibodies, which were affinity-purified by adsorbtion to immobilized Na^+ channel α subunits (Wollner & Catterall, 1986), were analyzed by recording Na^+ currents of rat muscle cells in the whole-cell voltage clamp configuration (Hamill et al, 1981; Gonoi et al, 1985). Rat skeletal muscle cells were dissociated from 20 day embryos, maintained in vitro for 4 days to allow fusion into

multinucleated myotubes, treated with colchicine to obtain round "myoballs", and studied after a total of 8 to 18 days in cell culture (Gonoi et al, 1985). The large size and spherical cell shape of the myoballs allowed us to obtain adequate voltage-clamp control and to perfuse antibody-containing solutions inside the cell under stable recording conditions.

Control experiments in the absence of antibodies (Fig. 12B, traces b and f) show no substantial changes in the kinetics of Na^+ currents in experiments that lasted as long as 180 min. However, when affinity-purified antibody to SP19 (Ab_{SP19}) was present in the pipet solution, a gradual slowing of Na^+ channel inactivation was observed over a period of several minutes as the antibody diffused into the cell (Fig. 12B, a and e). Intracellular application of antibodies to SP1, SP11, and SP20 had no effect on Na^+ currents under identical conditions (Fig. 12B, traces c, d, and g), suggesting that the effects of Ab_{SP19} were caused by direct interaction with the SP19 segment of the Na^+ channel α subunit.

The specifi ity of the antibody-induced modification of Na^+ currents was tested further by using the SP19 peptide to block the immunoreactivity of Ab_{SP19} (Fig. 13A). Affinity-purified antibodies to SP19 induced a significant slowing of the declining phase of Na^+ currents in about 20 min. At a test potential of -20 mV, the time constant for Na^+ channel inactivation increased from 2.3 to 4.4 msec (Fig. 13A, panel a). Under the same conditions, no time-dependent changes in Na^+ currents were found in control experiments in absence of antibody (Fig. 13A, panel b). After pretreatment of the affinity-purified Ab_{SP19} with the corresponding peptide (Gordon et al, 1987; Gordon et al, in press; Merrick & Catterall, unpublished results), a nearly complete block of the effect of the antibody on Na^+ channel inactivation was observed (Fig. 13A, panel c). These experiments provide strong evidence that the effect of the Ab_{SP19} on Na^+ channel inactivation result from its binding to the corresponding segment of the Na^+ channel α subunit.

The effects of Ab_{SP19} on Na^+ channel function were quite specific. No reproducible changes in Na^+ current amplitude under the influence of Ab_{SP19} could be detected. No substantial shifts in current-voltage relations due to the influence of Ab_{SP19} were observed (Fig. 13B). In some individual experiments, slight (2 to 4 mV) shifts of the voltage dependence of steady state Na^+ channel inactivation toward more negative membrane potentials were observed. However, statistical analysis of pooled data from five experiments did not reveal a significant shift of the inactivation curve in the presence of Ab_{SP19} (Fig. 13C).

The effect of the test pulse potential used to elicit Na^+ channel activation upon the antibody-induced slowing of Na^+ channel inactivation was examined. Figure 3 shows the effect of affinity-purified Ab_{SP19} on Na^+ currents recorded at four different test potentials. At each potential, traces taken before and after the onset of the antibody effect have been superimposed. For small depolarizations (for example, to -60 mV), no change in the time course of the Na^+ current occurs, as indicated by the coincidence of the two current traces in Fig. 14D. Inactivation of Na^+ currents recorded during test pulses to potentials equal to or more positive than -50 mV is slowed after application of antibody (Fig. 14C). For a test pulse to -30 mV, the time constant of Na^+ current decay is increased approximately two-fold, from 3.5 msec to 7.2 msec (Fig. 14B). During test pulse potentials to +90 mV (Figure 14A), the antibody-induced slowing of the inactivation is much more prominent than at negative test potentials. Such voltage-dependent effects are observed on the first depolarization after a prolonged period of inactivity, ruling out a dependence on stimulus frequency. The rising phase of the Na^+

current remained unaffected at all test potentials examined, indicating a high degree of specificity of the antibody effect for the inactivation process.

Na^+ channels bind α scorpion toxins and sea anemone toxins, which act at an extracellular site and specifically slow Na^+ channel inactivation (Catterall, 1980; Strichartz et all, 1985; Meves et al, 1985). The binding of these toxins is voltage-dependent with higher affinity at more negative membrane potentials (Catterall, 1977; Catterall, 1979). To assess the voltage dependence of binding of the Ab_{SP19}, we have examined the rate of modification of the Na^+ current decay at two holding potentials, -70 mV and -110 mV. The slowing of the Na^+ current decay occurs three times as fast at the more negative membrane potential (Fig. 15). No changes in inactivation kinetics were observed in control experiments. Evidently, the binding of SP19 antibodies to their site of action on the Na^+ channel is more rapid at negative holding potentials at which the Na^+ channels are not inactivated.

Our results indicate that Ab_{SP19} can provoke a substantial slowing of Na^+ channel inactivation by binding to the corresponding amino acid sequence in the proposed intracellular segment between homologous domains III and IV (Fig. 12A). Because Ab_{SP19} is active from inside the cell, these results confirm the assignment of this segment of the α subunit to the intracellular side of the membrane. In addition, our experiments provide direct evidence for a role of this intracellular peptide segment in Na^+ channel inactivation. A molecular model of Na^+ channel function has been proposed that also assigns an important role in inactivation to this peptide segment (Guy, in press). Further experimental evidence is required before the mechanism by which this peptide segment participates in channel inactivation can be defined.

The voltage dependence of the binding and action of Ab_{SP19} is of particular interest. The more rapid action of the antibody at a holding potential of -110 mV in comparison with that at -70 mV may result from increased accessibility of the corresponding segment of the α subunit to the antibody in the resting state of the channel as compared to the inactivated state, since Na^+ channels in rat muscle cells are 80% inactivated over this voltage range (Fig. 13C). This suggests a direct participation of this peptide segment in the protein conformational changes that lead to channel inactivation. Similarly, the removal of Na^+ channel inactivation by intracellular perfusion with proteases is also more rapid at negative holding potentials (for example, -110 mV) compared to more positive potentials (for example, -30 mV) (Salgado et al, 1985). The site of action of proteases in removing Na^+ channel inactivation may therefore be in or near the SP19 segment of the α subunit. It is noteworthy that Ab_{SP19} slows inactivation, but does not cause removal of inactivation as observed with proteases (Armstrong et al, 1973; Eaton et al, 1978; Oxford et al, 1978; Patlak & Horn, 1982). Ab_{SP19} remains bound to Na^+ channels for several minutes to hours as shown in biochemical experiments (Gordon et al, 1987; Gordon et al, in press; Merrick & Catterall, unpublished results). Therefore, our findings are most consistent with the view that Ab_{SP19} may bind to the corresponding peptide segment of the α subunit and impede its movement, in contrast to the proteases, which damage the structure.

In contrast to the dependence of the binding of Ab_{SP19} on holding potential, the dependence of the action of Ab_{SP19} on the test potential occurs too rapidly to be due to voltage-dependent binding. It is more likely that the preferential slowing of Na^+ current decay at more positive membrane potentials reflects a specific action of the antibodies on pathways of Na^+ channel gating that are particularly important in determining Na^+ current time course at more positive membrane potentials. For example, both single channel recording and gating current experiments suggest that the time course of Na^+ current decay at more negative potentials is controlled primarily by a slow rate of channel

entry to the activated state, while it is controlled by the inactivation process at more positive potentials (Aldrich et al, 1[illegible]; Aldrich & Stevens, 1987; Armstrong & Bezanilla, 1977; Bezanilla & Armstrong, 1981). In any case, our results imply that there are multiple conformational pathways between the resting and inactivated states, as proposed in most recent models of Na^+ channel gating (Aldrich et al, 1983; Aldrich & Stevens, 1987; Armstrong & Bezanilla, 1977; Bezanilla & Armstrong, 1981; Vandenberg & Horn, 1984; Gonoi & Hille, 1987), and suggest that Ab_{SP19} will be a valuable experimental tool to probe the involvement of the corresponding intracellular segment of the Na+ channel in these pathways.

All of the antibodies that have been tested on Na^+ channels in rat muscle cells in this study are directed against segments of the α subunits of rat brain R_{II} Na^+ channels. At present, the amino acid sequence of rat skeletal muscle Na^+ channel α subunits is not known, and it is uncertain whether the SP1, SP11, SP19, and SP20 peptide segments are identical for skeletal muscle Na^+ channels. The amino acid sequences of the SP19 segment of rat brain and eel electroplax Na^+ channels are identical (Noda et al, 1984; Noda et al, 1986b), and Ab_{SP19} recognizes Na^+ channel α subunits in skeletal muscle, heart, electroplax, and insect nervous system (Gordon et al, 1987; Gordon et al, in press; Merrick & Catterall, unpublished results), suggesting that the SP19 peptide segment is highly conserved in a wide range of Na^+ channel subtypes in different species. Moreover, the exponential time course of Na^+ current decay at -20 mV in the presence and absence of Ab_{SP19} suggests that the inactivation of both tetrodotoxin-sensitive and tetrodotoxin-insensitive Na^+ channels, which function in parallel in cultured rat muscle cells (Gonoi et al, 1985; Weiss & Horn, 1986; Ruppersberg et al, 1987), is slowed by Ab_{SP19}. The strong conservation of the amino acid sequence and functional effects of the SP19 peptide are consistent with an important role in rapid Na^+ channel inactivation, which is a conserved function of most Na^+ channels. The peptide segments corresponding to SP1, SP11, and SP20 are less well conserved and therefore may differ significantly in the α subunit of the skeletal muscle Na^+ channel.

In a previous study, it has been found that antibodies directed against a peptide corresponding to a proposed transmembrane segment containing amino acid residues 210 to 223 of the sequence of eel electroplax Na+ channel increase the rate of activation and inactivation of slow Na+ channels and shift the voltage dependence of inactivation of both slow and fast Na+ channels when applied to the extracellular surface of dorsal root ganglion cells (Meiri et al, 1987). Those results indicate that the process of Na^+ channel inactivation can be modified from the extracellular surface of the molecule by antibodies as well as by polypeptide neurotoxins from scorpions, sea anemones, coral and snail (Catterall, 1980; Strichartz et al, 1985; Meves et al, 1985; Catterall, 1988). Additional site-directed antibody probes may allow more complete mapping of the Na+ channel segments on both intracellular and extracellular surfaces that are involved in inactivation.

FIGURE 1

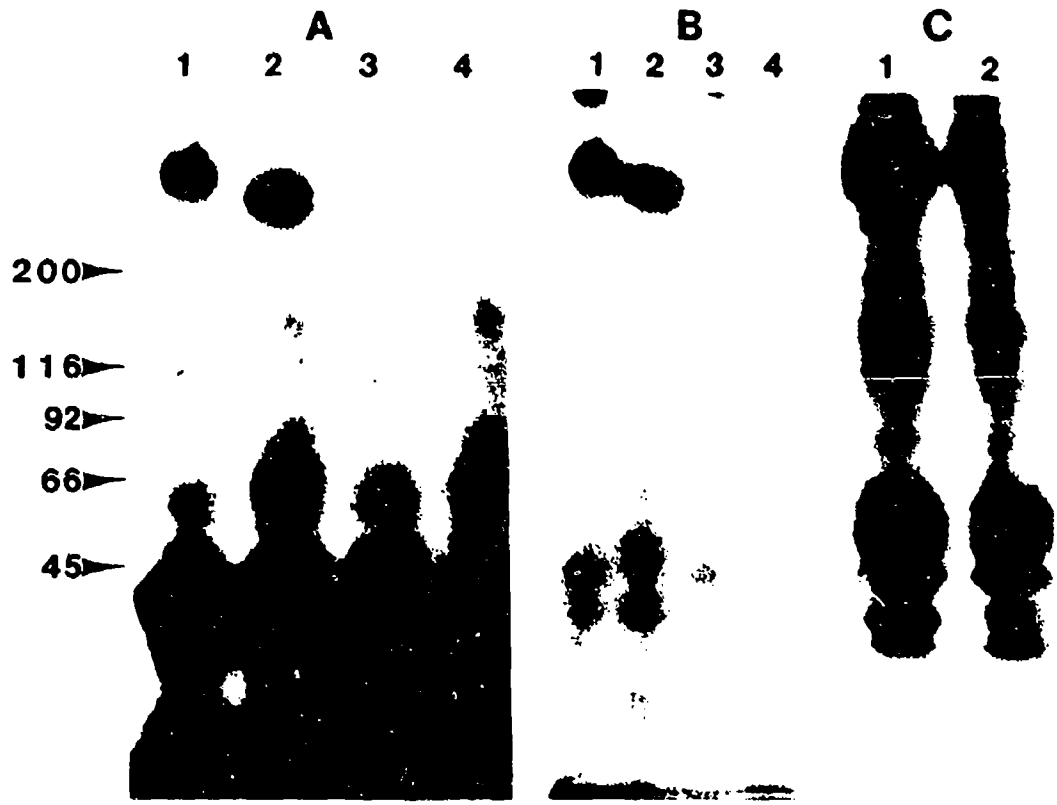

Figure 1. ***Photoaffinity labeling of the sodium channel in synaptosomes.*** **A.** Synaptosomes were photolabeled with ANB-^{125}I-LqTx as described under Experimental Procedures in the absence (lanes 1 and 2) or presence (lanes 3 and 4) of 400 nM native LqTx. Samples were analyzed by SDS-PAGE in 7-20% linear gradient polyacrylamide gels (Messner and Catterall, 1985) under non-reducing (lanes 1 and 3) or reducing (lanes 2 and 4) conditions, and radiolabeled protein bands were visualized by autoradiography. **B.** A similar experiment was carried out with MAB-^{125}I-LqTx as described under Experimental Procedures. **C.** Synaptosomes were photolabeled with MAB-^{125}I-LqTx prepared using a 250-fold excess of MABI over amino residues in the coupling reaction in the absence (lane 1) or presence (lane 2) of 400 nM LqTx.

FIGURE 2

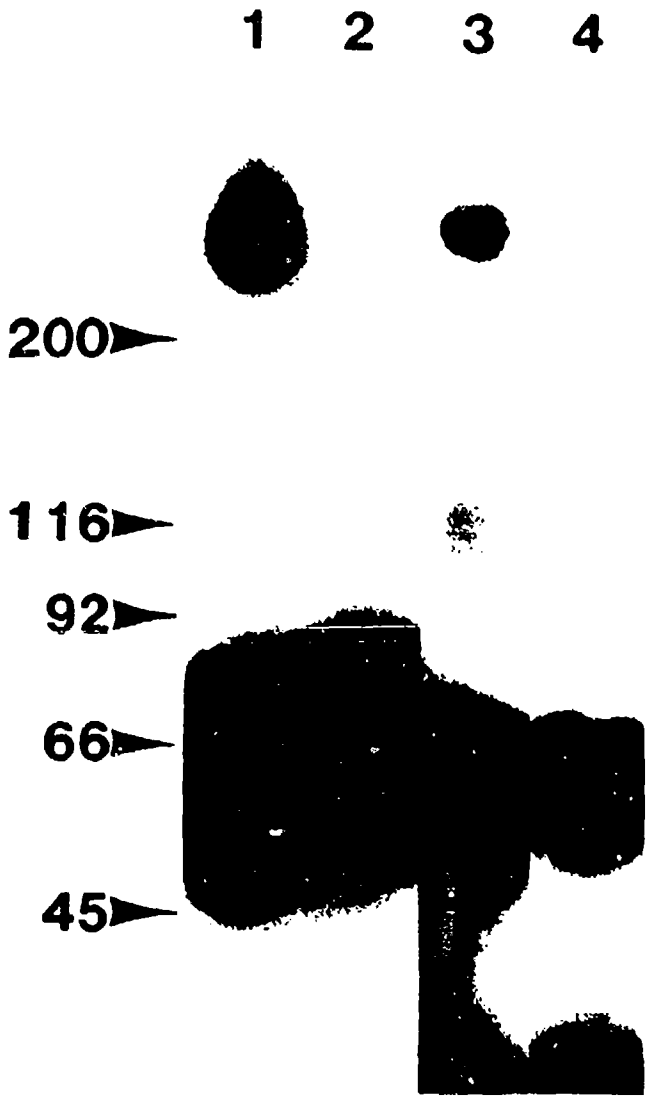

Figure 2. ***Photoaffinity labeling of purified and reconstituted sodium channels.*** Purified and reconstituted sodium channels were photoaffinity labeled with ANB-^{125}I-LqTx (lanes 1 and 2) and MAB-^{125}I-LqTx (lanes 3 and 4) in the absence (lanes 1 and 3) or presence (lanes 2 and 4) of 400 nM LqTx. The samples were analyzed by SDS-PAGE under reducing conditions as described in the legend to Fig. 1.

FIGURE 3

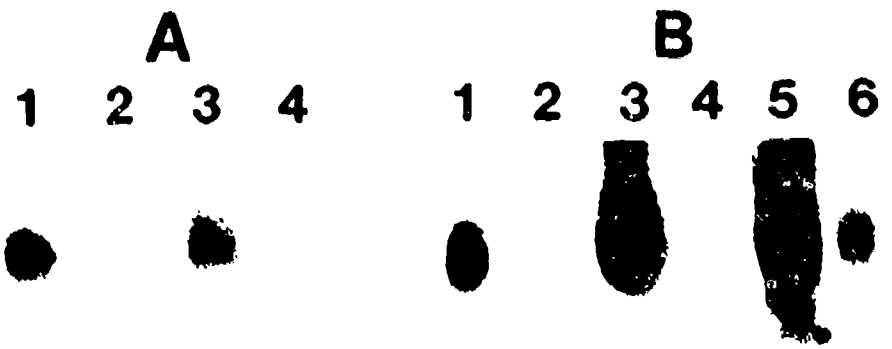

Figure 3. ***Immunoprecipitation of photolabeled sodium channels with subtype-specific antibodies.*** A. Synaptosomes (75 ml of 1.67 mg/ml) were photoaffinity labeled with ANB-LqTx and solubilized in Triton X-100 as described under Experimental Procedures. Sodium channels were incubated with 20 µl of affinity-purified anti-$SP11_I$ (lane 1), affinity-purified anti-$SP11_I$ that had been blocked by incubation with excess $SP11_I$ peptide (lane 2), affinity-purified anti-$SP11_{II}$ antibodies (lanes 3), or affinity-purified anti-$SP11_{II}$ antibodies that had been blocked by incubation with excess $SP11_{II}$ in Buffer S plus 1 mg/ml BSA at 4°C overnight. One mg of protein A-Sepharose per µl of serum was added from a 10% (w/v) suspension prepared in the same solution. The samples were mixed by rotation at 4°C for 30 min. Supernatants were removed and the pellets were washed twice with 10 volumes of Buffer S containing 4 mg/ml BSA and once with 5 volumes of the same solution without BSA. Immunoprecipitated proteins were finally removed fron the pellet by incubation with SDS-PAGE loading solution at 100°C for 2 min, and the samples were analyzed by SDS-PAGE and autoradiography. B. Purified and reconstituted sodium channels were photoaffinity labeled with ANB-LqTx and purified by WGA-Sepharose chromatography. Samples containing 40 fmol of the photolabeled sodium channel in 15 µl were immunoprecipitated with 20 µl of anti-$SP11_I$ antibodies (lane 1), anti-$SP11_I$ antibodies that had been blocked by incubation with excess $SP11_I$ peptide (lane 2), anti-$SP11_{II}$ antibodies (lane 3), anti-$SP11_{II}$ antibodies that had been blocked by incubation with excess $SP11_{II}$ peptide (lane 4), anti-β2 subunit-specific antibodies without reduction of disulfide bonds (lane 5), or anti-β2 subunit-specific antibodies after reduction of disulfide bonds (lane 6) as described for panel A. The resulting immunoprecipitates were solubilized and analyzed by SDS-PAGE and autoradiography.

FIGURE 4

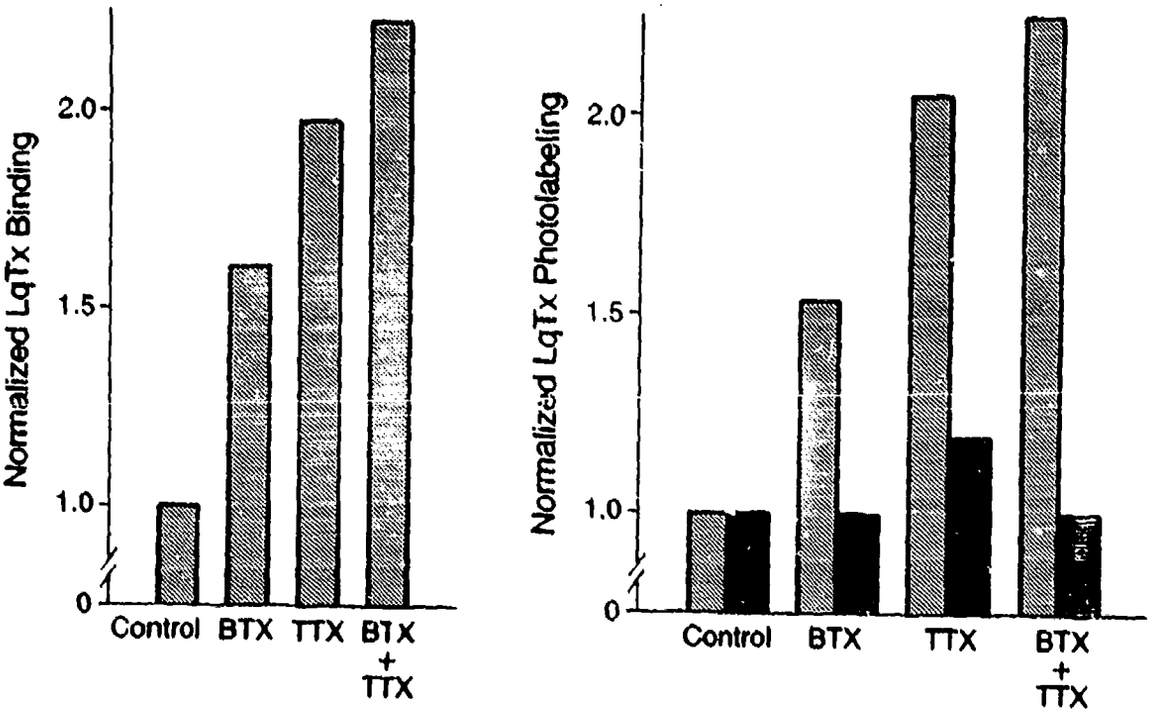

Figure 4. ***Modulation of LqTx binding and photolabeling by neurotoxins acting at receptor sites 1 and 2.*** **A.** Specific binding of 0.5 nM ^{125}I-LqTx to purified and reconstituted sodium channels was measured as described under Experimental Procedures without further additions or in the presence of 1 μM TTX, 2 μM BTX or both 1 μM TTX and 2 μM BTX. **B.** Purified and reconstituted sodium channels were photolabeled with LqTx as described under Experimental Procedures without further additions or in the presence of 1 μM TTX, 2 μM BTX, or both 1 μM TTX and 2 μM BTX. The samples were analyzed by SDS-PAGE and autoradiography, and the incorporation of ^{125}I-LqTx into the α subunits was determined by gamma counting.

FIGURE 5

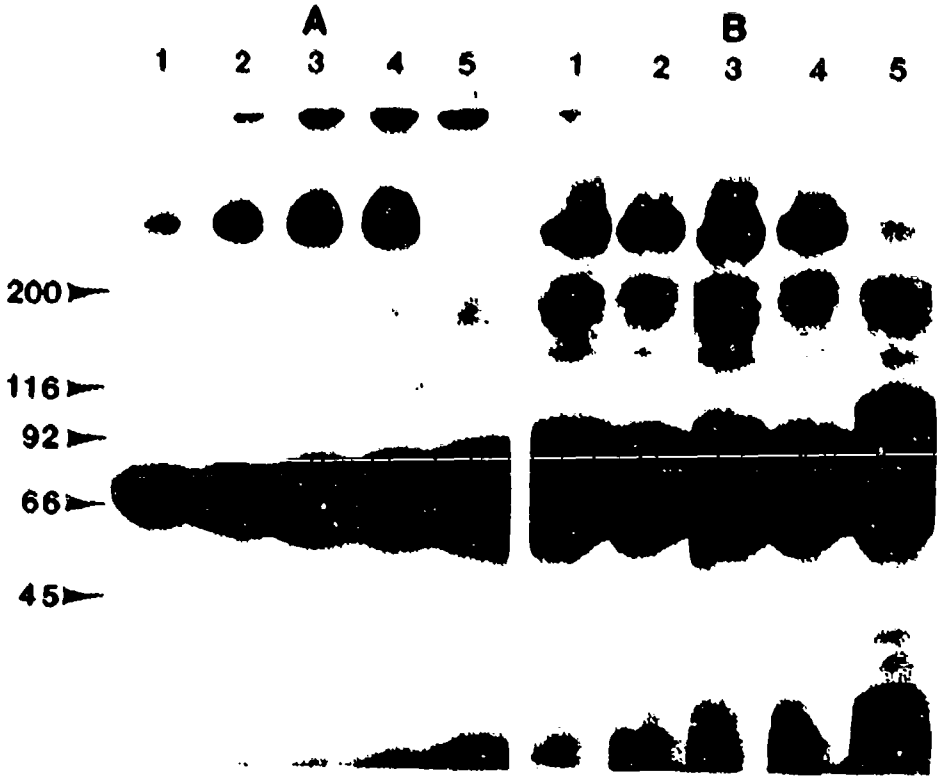

Figure 5. ***Effect of neurotoxins acting at receptor sites 1 and 2 on photolabeling of the sodium channel by LqTx.*** **A.** Purified and reconstituted sodium channels were photolabeled with ANB-^{125}I-LqTx as described under Experimental Procedures without further additions (lane 1) or in the presence of 1 mμ BTX (lane 2), 1 μM TTX (lane3), 1 μM BTX plus 1 μM TTX (lane 4), and 400 nM LqTx (lane 5). The samples were analyzed by SDS-PAGE and autoradiography. **B.** A similar experiment was carried out with MAB-^{125}I-LqTx.

FIGURE 6

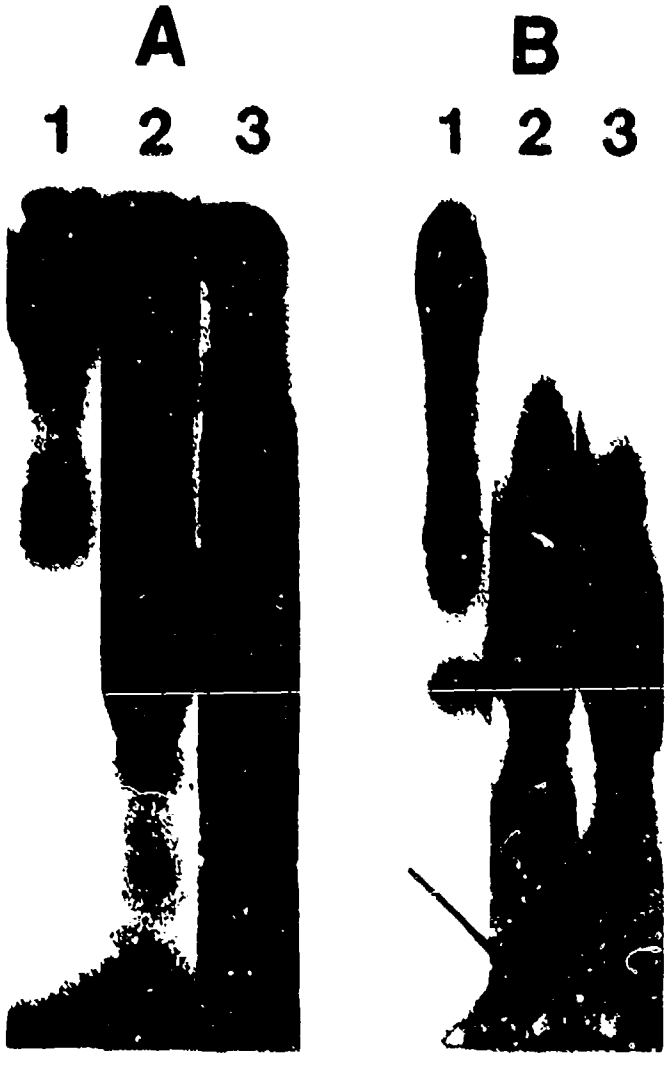

Figure 6. ***Proteolysis of the photolabeled α-subunit.*** **A.** Purified and reconstituted sodium channels were photolabeled with ANB-^{125}I-LqTx as described under Experimental Procedures. Alpha subunits (150 µl of 25 nM) were incubated at 37°C for 20 min without further additions (lane 1), or with 50 µg/ml of *S. aureus* V8 protease (lane 2), or 25 µg/ml of chymotrypsin (lane 3). The samples were analyzed by SDS-PAGE in 6-20% linear gradient polyacrylamide gels. **B.** A similar experiment was carried out with α-subunits photolabeled with MAB-^{125}I-LqTx.

FIGURE 7

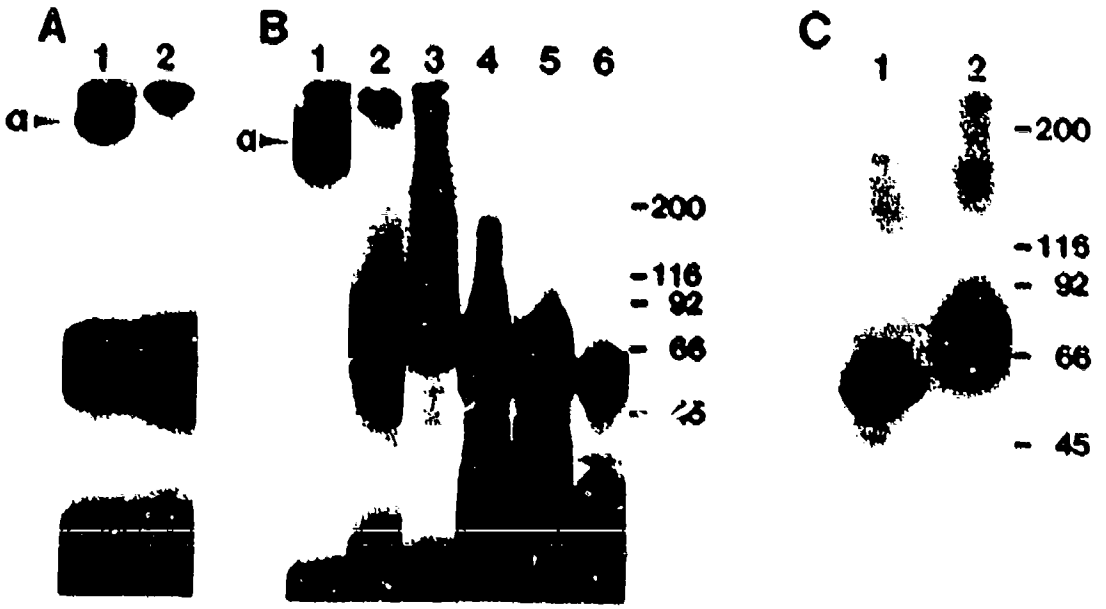

Figure 7. ***Isolation of a glycosylated 48 kDa α subunit fragment containing covalently attached LqTx.*** A. Twenty µl of solution containing purified and reconstituted sodium channels were photolabeled in the absence (lane 1) or presence (lane 2) of 1 µM LqTx and analyzed by $NaDodSO_4$-PAGE using gel system B. Radiolabeled protein bands were visualized by autoradiography. **B.** Thirty µl of solution containing photoaffinity labeled sodium channel purified by WGA-Sepharose affinity chromatography were incubated at 37°C for 20 min with no protease treatment (lane 1), 30 µg/ml α-chymotrypsin (lane 2), 150 µg/ml *S. aureus* protease V8 (lane 3), 5 µg/ml elastase (lane 4), 5 µg/ml TPCK-trypsin (lane 5), and 50 µg/ml of thermolysin (lane 6) in a final volume of 100 µl of Buffer S containing 0.5% Triton X-100. The reaction was stopped by addition of concentrated $NaDodSO_4$-PAGE sample loading solution and immediate incubation at 100°C for 2 min. The samples were analyzed by $NaDodSO_4$-PAGE in gel system B. C. One hundred µl samples containing photolabeled sodium channels digested by protease V8 (Fig. 1B, lane 5) were mixed with 7 µl of 10% $NaDodSO_4$ and incubated at 100°C for 2 min. The concentration of Triton X-100 was increased to 1.5%. After incubation at 0°C for 1 hr, samples were desalted by rapid gel filtration using Sephadex G-50 columns equilibrated in Buffer S containing 0.5% Triton X-100 and 0.1 mg/ml BSA. The samples were finally incubated at 0°C for 1 hr in the presence (lane 1) or absence (lane 2) of 0.5 units of neuraminidase. Samples were analyzed by $NaDodSO_4$-PAGE in gel system A and the photolabeled protein bands were visualized by autoradiography.

FIGURE 8

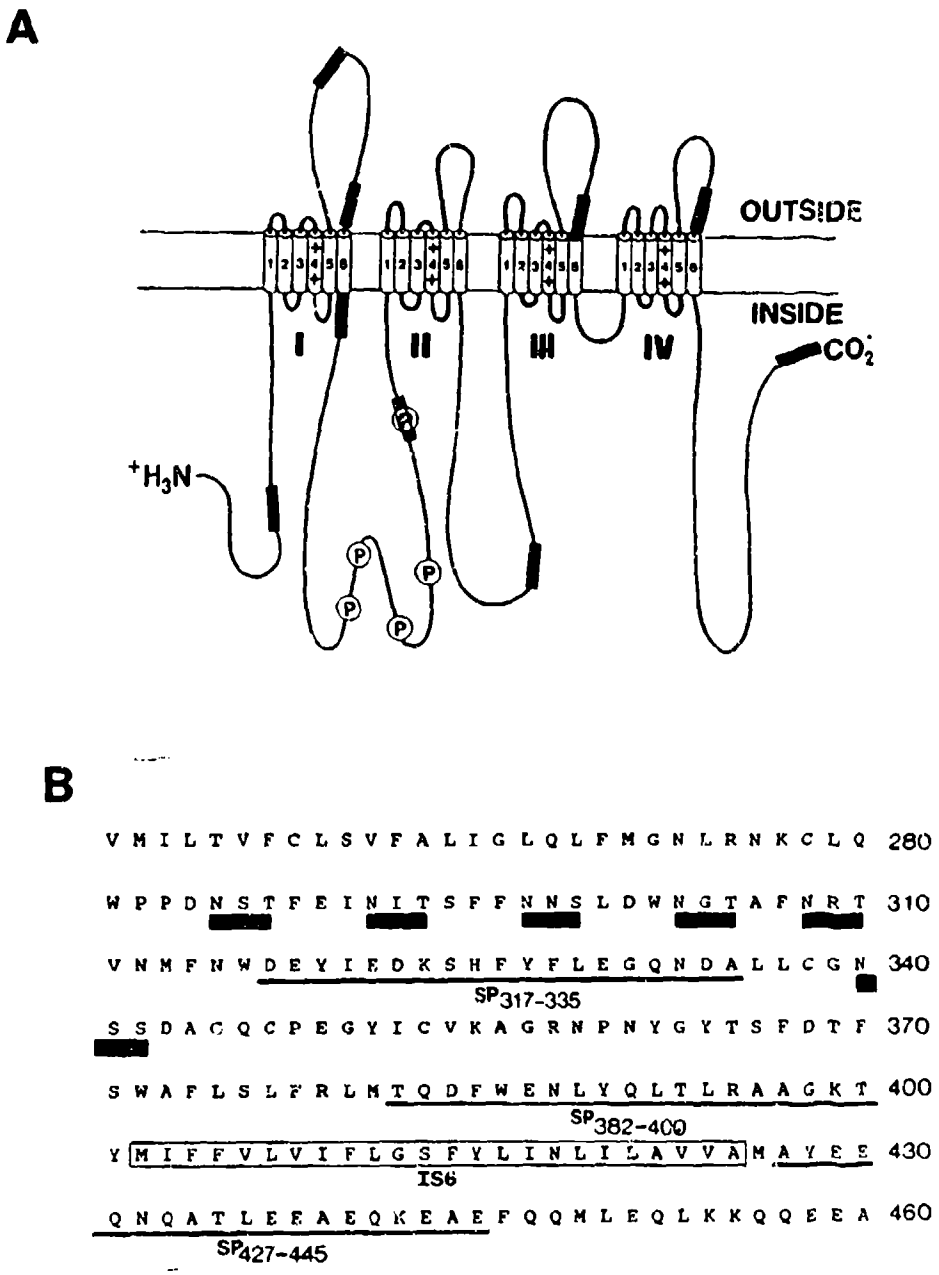

Figure 8. ***Structure of the α subunit of the R_{II} sodium channel.*** **A.** Transmembrane folding model of the α subunit of the rat brain sodium channel (6) showing the approximate location of the segments of the amino acid sequence (1, SP_{31-47}; 2, $SP_{317-335}$; 3, $SP_{382-400}$; 4, $SP_{427-445}$; 5, $SP_{676-690}$; 6, $SP_{1106-1125}$; 7, $SP_{1430-1448}$; 8, $SP_{1729-1748}$; and 9, $SP_{1988-2005}$) that were used to raise antipeptide antibodies and sites of *in vivo* phosphorylation by cAMP-dependent protein kinase (38). **B.** Detail of the primary structure of the region surrounding the site of covalent attachment of LqTx. Filled boxes underline potential N-linked glycosylation sites; bold lines underline sites of binding of three anti-peptide antibodies; open box encloses the proposed transmembrane segment S6.

FIGURE 9

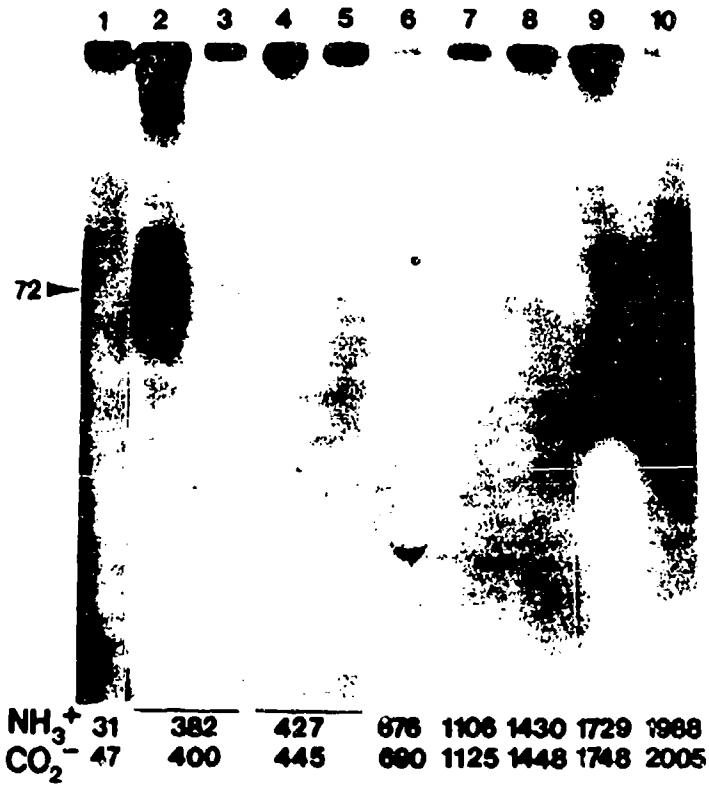

Figure 9. ***Immunoprecipitation of proteolytic fragments of photolabeled αβ2 with sequence-specific antibodies.*** Samples (150 µl) of photolabeled αβ2 were cleaved with protease V8 as described in Fig. 1C and incubated overnight at 4°C with 15 µl of different sequence-specific antibodies. The numbers under each lane correspond to the amino (NH_3^+) and carboxyl (CO_2^-) termini of the α subunit segment against which the antibody was raised. Immunoprecipitation was carried out as described under Experimental Procedures, the samples were analyzed by $NaDodSO_4$-PAGE in gel system A, and radiolabeled protein bands were visualized by autoradiography. In the samples in lanes 3 and 5, 5 nmol of the corresponding peptide were added together with the antibody to block specific immunoprecipitation.

FIGURE 10A

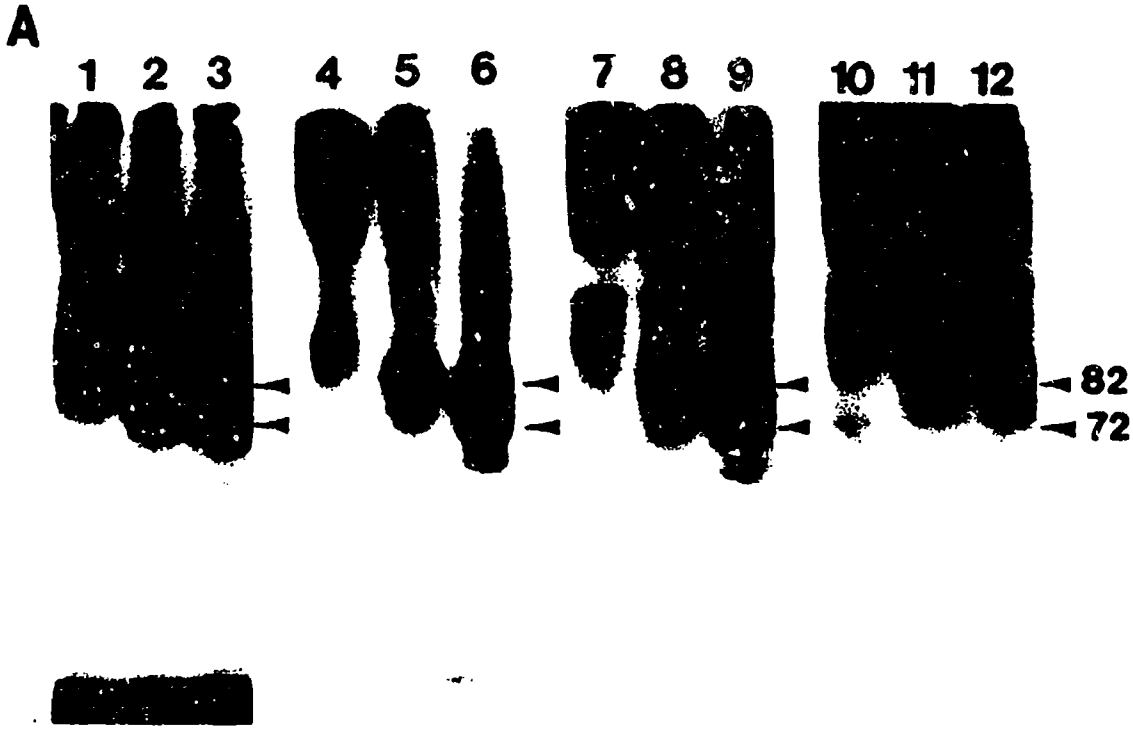

Figure 10. ***Immunoprecipitation of partial proteolytic fragments of photolabeled αβ2 with sequence-specific antibodies.*** **A.** Samples (100 µl) of photolabeled αβ2 (Fig. 1B, lane 1) in Buffer S containing 0.1% Triton X-100 were incubated at 37°C for 25 min in the presence of 7.5 µg/ml (lanes 1, 4, 7, and 10), 32 µg/ml (lanes 2, 5, 8, and 11), and 150 µg/ml (lanes 3, 6, 9, and 12) of *S. aureus* V8 protease. After stopping the digestion and desalting as in Fig. 1C, the samples were analyzed by $NaDodSO_4$-PAGE in the gel system B (lanes 1-3) or immunoprecipitated with 15 µl of sequence-specific antibodies and analyzed by $NaDodSO_4$-PAGE: lanes 4-6, anti-$SP_{317-335}$; lanes 7-9, anti-$SP_{382-400}$; lanes 10-12, anti-$SP_{427-445}$. Photolabeled protein bands were visualized by autoradiography. **B.** Samples (125 µl) of photolabeled αβ2 were incubated at 0°C for 2.5 hr with 0.5 units of neuraminidase and then for 25 min at 37°C with 1 µg/ml (lanes 1, 4, 7, and 10), 10 µg/ml (lanes 2, 5, 8, and 11), and 100 µg/ml (lanes 3, 6, 9, and 12) of TPCK-trypsin. After stopping the digestion and desalting as in Fig. 1C, the samples were analyzed by immunoprecipitation and $NaDodSO_4$-PAGE as in panel A.

FIGURE 10B

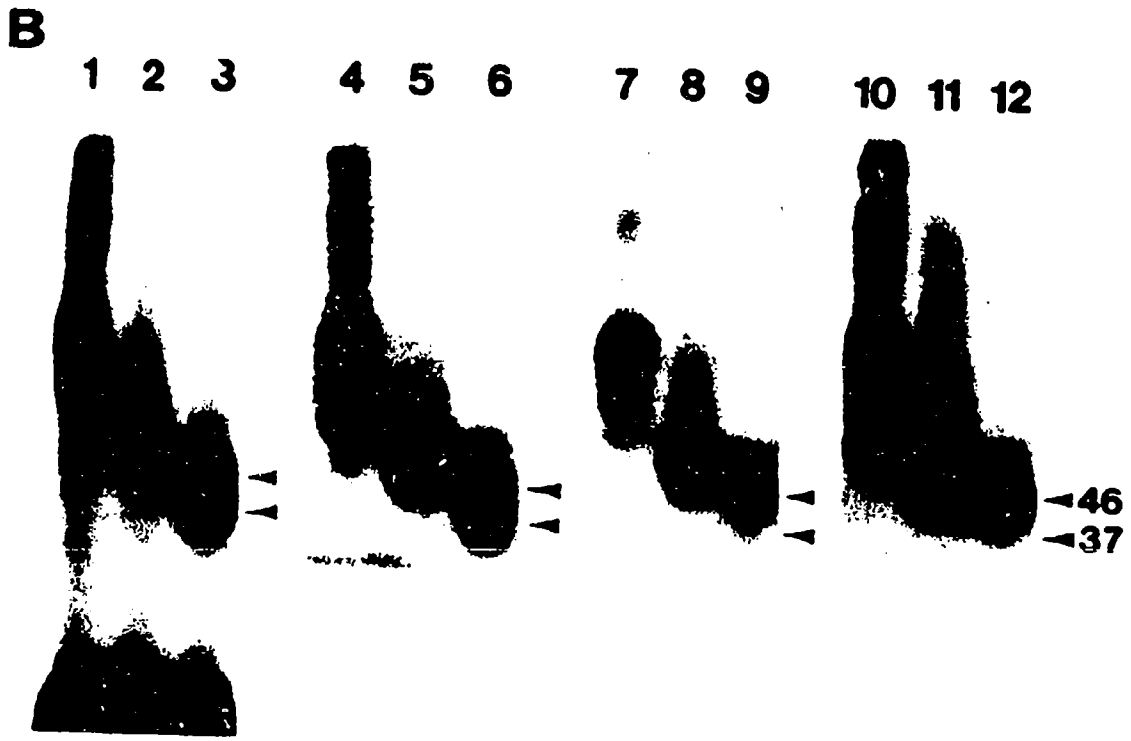

FIGURE 11

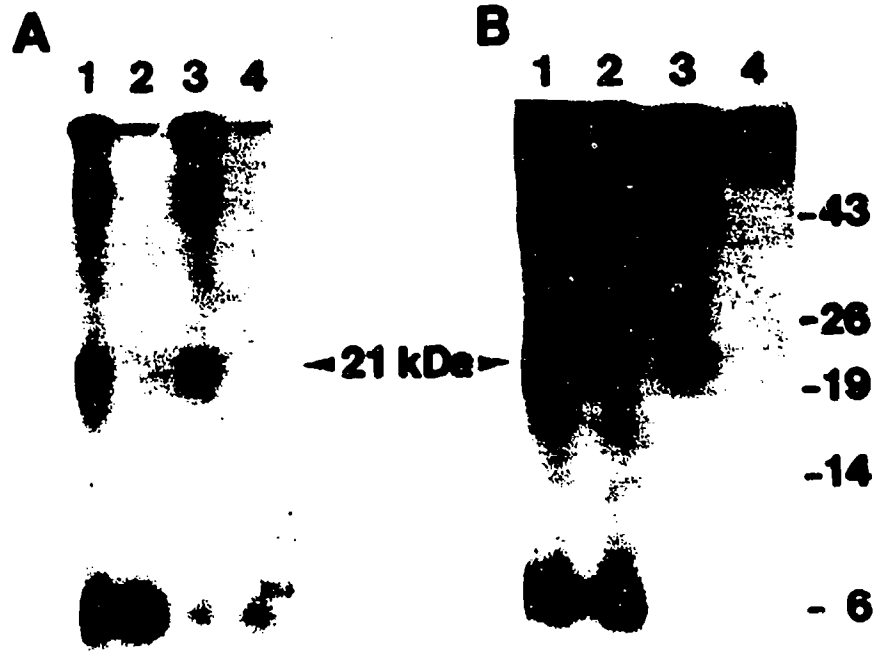

Figure 11. ***Immunoprecipitation of CNBr fragments of photolabeled αβ2 with sequence-specific antibodies.*** A. Samples (300 µl) of photolabeled αβ2 in Buffer S containing 0.1% Triton X-100 were incubated at 37°C for 25 min in the presence of 10 µg/ml of TPCK-trypsin. The reaction was stopped by addition of $NaDodSO_4$ and 2-mercaptoethanol to final concentrations of 0.7% and 10 mM respectively, the reaction medium was incubated at 100°C for 2 min, iodoacetamide was added to a final concentration of 15 mM, and the samples were incubated for an additional hour at room temperature and finally desalted by rapid gel filtration on Sephadex G-25 columns equilibrated in 0.2% $NaDodSO_4$. The material obtained in this way was digested at room temperature for 20 hr with 1% CNBr in 70% formic acid. At the end of the digestion, the solution was evaporated to dryness under vacuum, and the residual solid was resuspended in 300 µl of 0.1 M ammonium acetate, pH 8.5, 0.1M β-mercaptoethanol and lyophilized. The final solid was redissolved in 160 µl of 75 mM sodium phosphate, pH 7.5. 25 µl aliquots were immunoprecipitated with 15 µl of sequence-specific antibodies and analyzed by SDS-PAGE in gel system C: lane 1, anti-$SP_{317-335}$; lane 2, anti-$SP_{317-335}$ previously blocked with peptide; lane 3, anti-$SP_{382-400}$; lane 4, anti-$SP_{382-400}$ previously blocked with peptide. Photolabeled protein bands were visualized by autoradiography. B. A similar experiment was carried out with 300 µl of photolabeled αβ2 which was desialylated by incubation with 1.5 units neuraminidase at 0°C for 2 hr prior to digestion with trypsin. These samples were then processed as described for panel A.

FIGURE 12

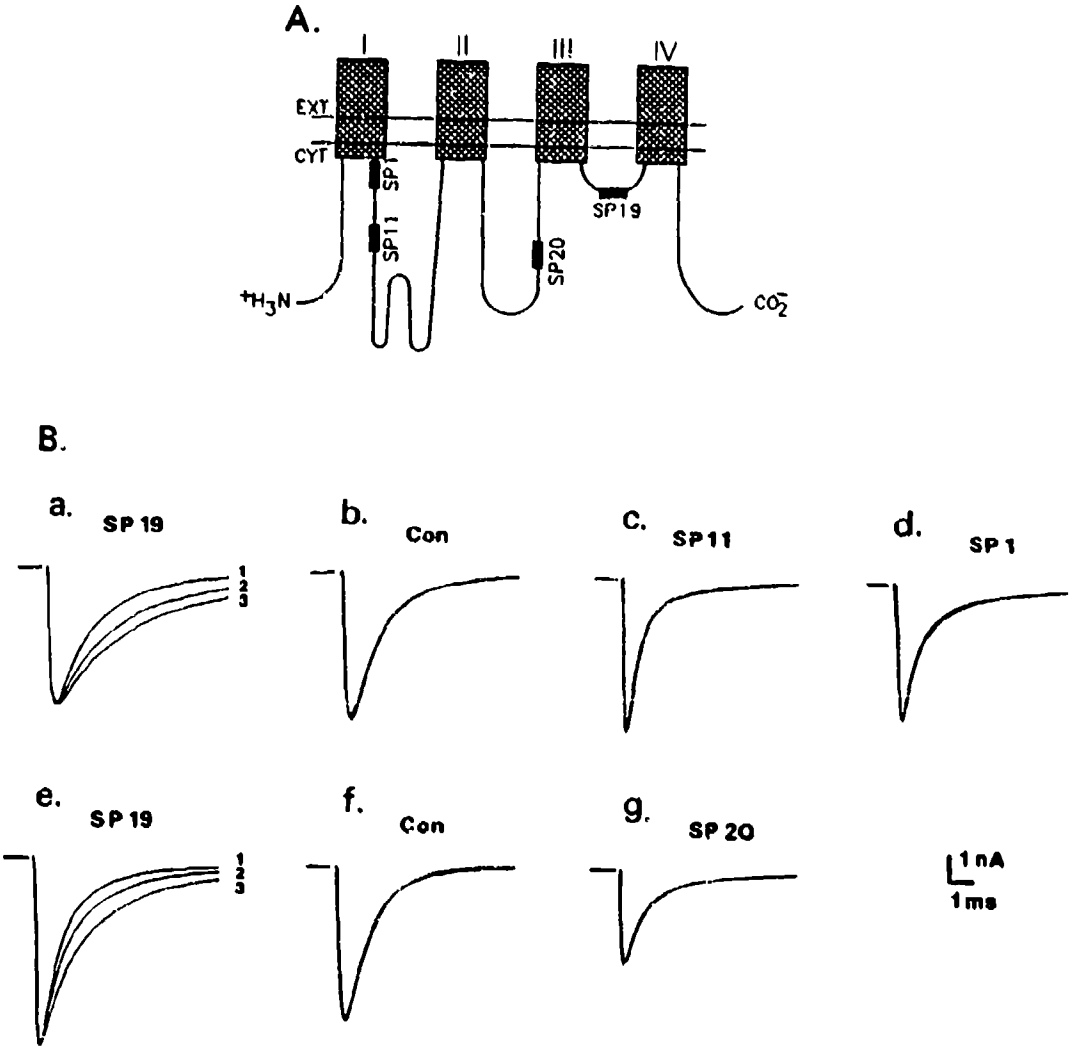

Figure 12. ***Functional effects of antibodies against segments of the proposed intracellular domains of the Na+ channel α subunit.*** (A) Schematic representation of the primary structure of Na^+ channel α subunit with designated peptide segments that are recognized by the four site-directed antibodies: SP1, SP11, SP20, and SP19. (B) Na^+ currents during intracellular exposure to different sequence-directed antibodies. Na+ currents were elicited from a holding potential of -70 mV or -110 mV by a 100-ms hyperpolarizing prepulse to -160 mV followed by a 9 ms test pulse to -5 mV. In each panel, two or three sequential Na+ current traces are presented at increasing times of exposure to the antibody solution in the recording pipet: a, anti-SP19 for 6 (trace 1), 12 (trace 2), and 23 (trace 3) min at -110 mV; b, control for 7 and 31 min at -110 mV; c, anti-SP11 for 4 and 26 min at -110 mV; d, anti-SP1 for 8 and 41 min at -110 mV; e, anti-SP19 for 8 (trace 1), 25 (trace 2), and 61 (trace 3) min at -70 mV; f, control for 8 and 68 min at -70 mV, and g, anti-SP20 for 7 and 60 min at -70 mV. Na+ current traces were normalized to allow direct comparison of time courses.

FIGURE 13

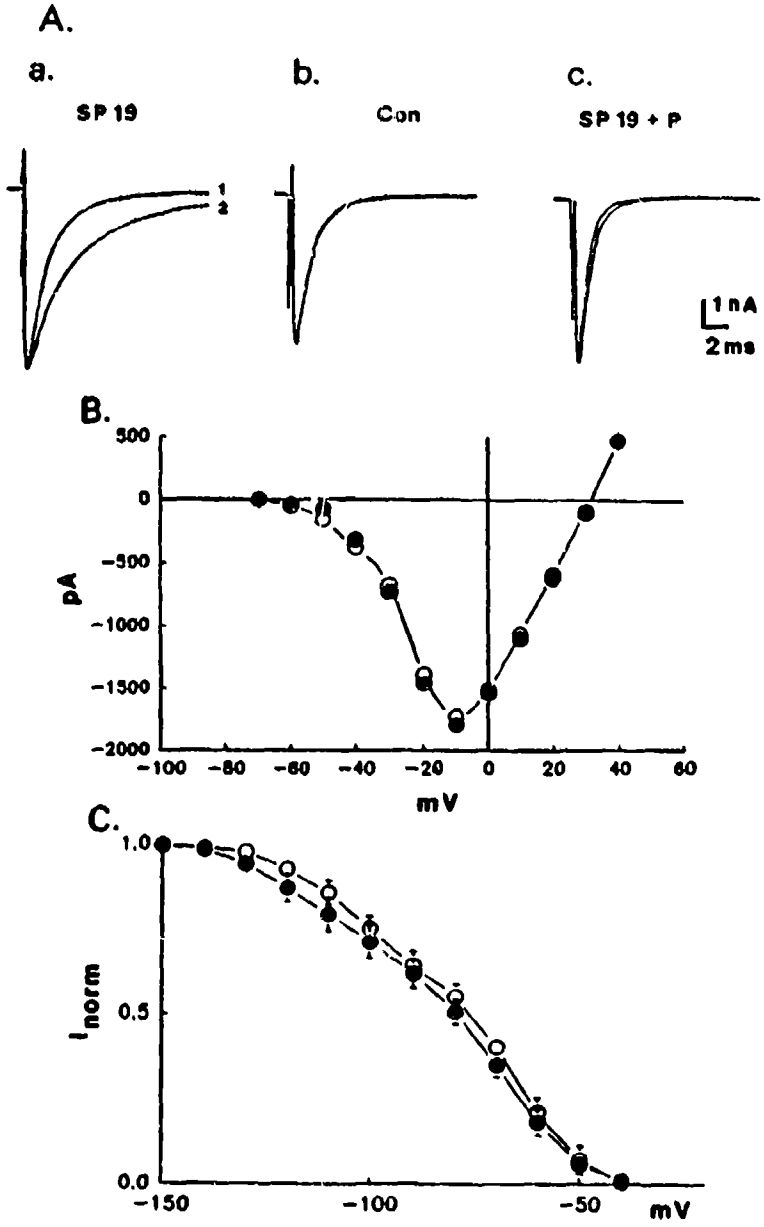

Figure 13. ***Specificity of the effects of antibodies to SP19 on Na^+ currents.*** (A) Whole cell Na^+ currents were recorded at the time intervals indicated below after breaking into the cell in intrapipet solutions containing no additions, Ab_{SP19}, or Ab_{SP19} that had been incubated with SP19 peptide (1 nmol/µl antibody solution) for 30 min at 0°C before addition to the recording pipette (7): **a**, anti-SP19 antibodies for 5 (trace 1) or 24 (trace 2) min; **b**, control solution for 5 and 33 min; and **c**, anti-SP19 antibodies previously incubated with SP19 peptide for 6 or 28 min. Cells were maintained at a holding potential of -110 mV, hyperpolarized to -140 mV for 100 msec, and then stimulated by a 16-msec test pulse to -20 mV to elicit Na^+ currents. (**B**) Current-voltage relations of Na^+ currents in the presence of affinity-purified Ab_{SP19} in the recording pipet. Whole cell Na^+ currents were measured after 7 ( ) and 57 ( ) min after breaking the cell membrane in the presence of anti-SP19 antibodies in the intrapipet solution. Cells were maintained at a holding potential of -70 mV, hyperpolarized to -120 mV for 40 msec, and depolarized to the indicated membrane potentials for 16 msec to elicit Na^+ currents. Peak Na^+ currents are plotted versus the test pulse potential. (C) Mean Na^+ current inactivation curves in the presence of Ab_{SP19}. Whole-cell Na^+ currents were measured for five cells at 3 to 8 min ( ) or 25 to 53 min ( ) after breaking the cell membrane in the presence of Ab_{SP19} in the intrapipet solution. Cells were maintained at a holding potential of -70 mV, changed to the indicated prepulse potentials for 100 msec, and depolarized to -5 mV for 9 msec to elicit Na^+ currents. Mean values $\pm$ SE from five experiments are plotted as a function of the applied prepulse potential.

FIGURE 14

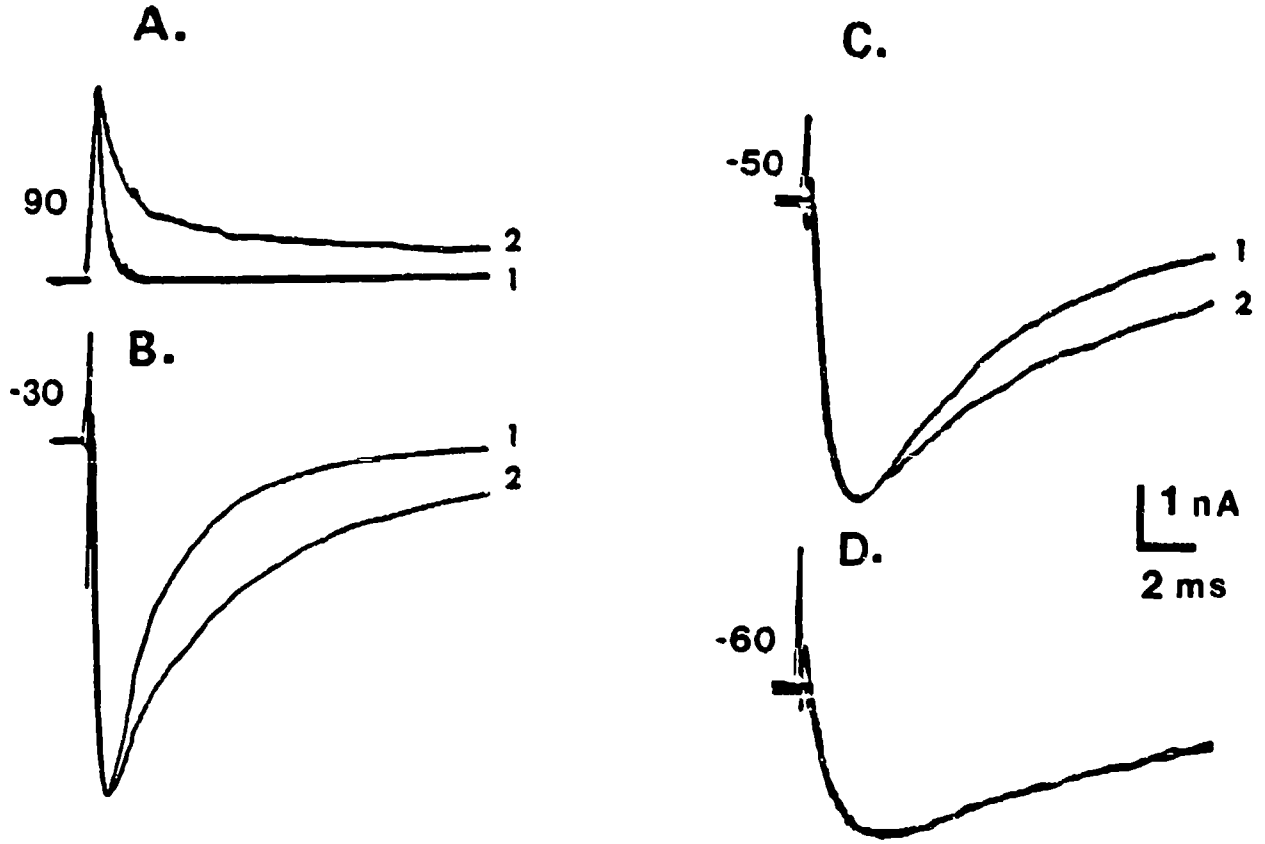

Figure 14. ***Voltage dependence of the effect of antibodies to SP19 on Na^+ currents.*** Whole-cell Na^+ currents were recorded at 5 (trace 1) or 24 (trace 2) min after breaking the cell membrane in the presence of Ab_{SP19} in the recording pipet. The cell was maintained at a holding potential of -110 mV, hyperpolarized to -140 mV for 100 msec, and depolarized to the indicated membrane potentials for 16 msec to elicit Na^+ currents.

FIGURE 15

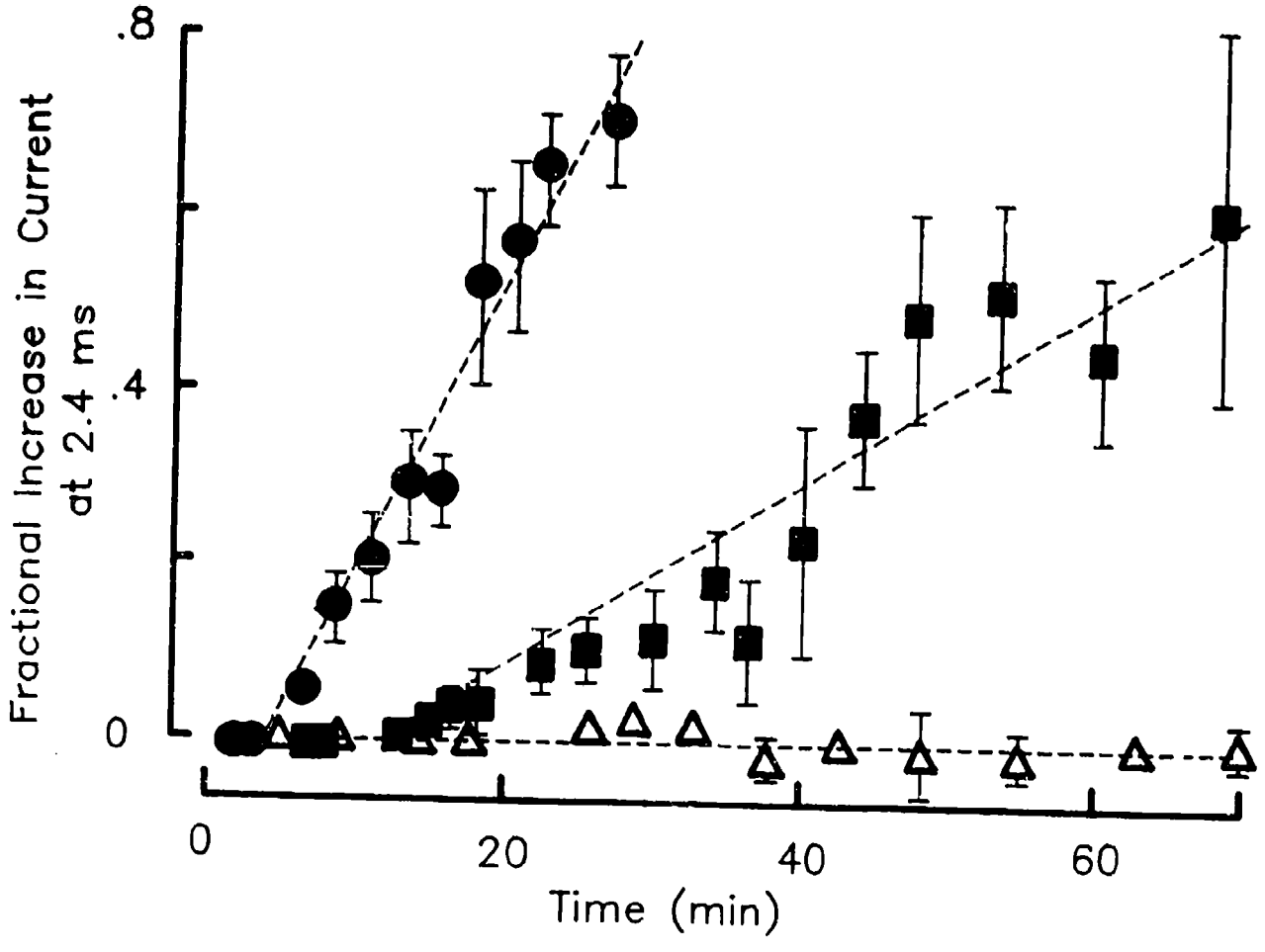

Figure 15. ***Voltage-dependence of the rate of action of Ab_{SP19}.*** Whole-cell Na^+ currents were recorded at the indicated times after breaking the cell membrane in the presence of control intrapipet solution ( ) at a holding potential of -110 mV, in the presence of Ab_{SP19} in the recording pipet at a holding potential of -110 mV ( ), or in the presence of anti-SP19 antibodies in the recording pipet at a holding potential of -70 mV ( ). Cells were hyperpolarized to -160 mV for 100 msec and depolarized to -5 mV for 9 msec to elicit Na^+ currents. The rate of slowing of inactivation by Ab_{SP19} was assessed by measuring the fraction of the Na^+ current that had not inactivated 2.4 msec after the beginning of the test pulse as a function of the time, t, after breaking the cell membrane. This fraction, $f_{2.4}$, was calculated from each set of Na^+ current records and the fractional increase in Na^+ current at 2.4 msec, $[f_{2.4}]/[f_{2.4}]_0 - 1$, was plotted on the ordinate as a function of the time (t) of exposure to Ab_{SP19}. $[f_{2.4}]_0$ was estimated from Na^+ current traces taken 1.5 to 5 min after breaking the cell membrane, before the antibody effect had begun. Mean values ± SEM from seven experiments in the presence of Ab_{SP19} and three experiments in the absence of antibody are presented.

REFERENCES

Agnew, W.S. (1984) *Annu. Rev. Physiol.* **46,** 517

Aldrich, R.W. and Stevens, C.F. (1987) *J. Neurosci.* **7,** 418.

Aldrich, R.W., Corey, D.P. and Stevens, C.F. (1983) *Nature* **306,** 436.

Armstrong, C.M. (1981) *Physiol. Rev.* **61,** 644.

Armstrong, C.M. and Bezanilla, F. (1977) *J. Gen. Physiol.* **70,** 567.

Armstrong, C.M., Bezanilla, F., and Rojas, E. (1973) *J. Gen. Physiol.* **62,** 375.

Auld, V.J., et al. (1988) *Neuron* **1,** 449-461.

Barchi, R.L. (1988) *Ann. Rev. Neurosci.* **11,** 455-495.

Barchi, R.L. (1984) *Trends Biochem. Sci.* **9,** 358.

Beneski, D. A. and Catterall, W. A. (1980) *Proc. Natl. Acad. Sci. USA* **77,** 639-643.

Bezanilla, F. and Armstrong, C.M. (1981) ibid., p. 549.Catterall, W. A. (1977) *J. Biol. Chem.* **252,** 8669-8676.

Catterall, W. A. (1979) *J. Gen. Physiol.* **74,** 375-391.

Catterall, W. A. (1980) *Ann. Rev. Pharmacol. Toxicol.* **20,** 15-43.

Catterall, W. A. (1984) *Science* **223,** 653-661.

Catterall, W. A. (1986) *Ann. Rev. Biochem.* **55,** 953-985.

Catterall, W. A. (1988) *ISI Atlas of Science: Pharmacol.* **2,** 190-195.

Catterall, W. A. and Risk, M. (1981) *Mol. Pharmacol.* **19,** 45-348.

Catterall, W. A., Morrow, C. S., and Hartshorne, R. P. (1979) *J. Biol. Chem.* **254,** 11379-11387.

Catterall, W.A. (1977) *J. Biol. Chem.* **252,** 8669.

Catterall, W.A. (1980) *Annu. Rev. Pharmacol. Toxicol.* **20,** 15.

Catterall, W.A. (1984) *Science* **223,** 653.

Catterall, W.A. (1986) *Annu. Rev. Biochem.* 55, 953.

Couraud, F., Jover, E., Dubois, J.M., and Rochat, H. (1982) *Toxicon.* **20,** 9-16.

Darbon, H., Jover, E., Couraud, F., and Rochat, H. (1983a) *Biochem Biophys. Res. Commun.* **115,** 415-422.

Darbon, H., Jover, E., Couraud, F., and Rochat, H. (1983b) *Int. J. Peptide Protein Res.* **22,** 179-186.

Eaton, D., Brodwick, M.S., Oxford, G.S., and Rudy, B. (1978) *Nature* **271,** 473.

El Ayeb, M., Bahraoui, E. M., Granier, C., and Rochat, H. (1986) *Biochemistry* **25,** 6671-6677.

Elmer, L.W., O'Brien, B.J., Nutter, T.J., and Angelides, K.J. (1985) *Biochemistry* **24,** 8128-8137.

Feller, D.J., Talvenheimo, J. A., and Catterall, W. A. (1985) *J. Biol. Chem.* **260,** 11542-11547.

Fontecilla-Camps, J. C., Almassy, R. J., Suddath, F. L., and Bugg, C. E. (1982) *Toxicon* **20,** 1-7.

Goldin, A.L. et al. (1986) *Proc. Natl. Acad. Sci. U.S.A.* **83,** 7503.

Gonoi, T. and Hille, B. (1987) *J. Gen. Physiol.* **89,** 253.

Gonoi, T., Sherman, S.J., Catterall, W.A. (1985) *J. Biol. Chem.* **5,** 2559.

Gordon, D., et al., (1987) *Proc. Natl. Acad. Sci. U.S.A.* **84,** 8682 .

Gordon, D., Merrick, D., Auld, V., Dunn, R., Goldin, A. L., Davidson, N., and Catterall, W. A. (1987) *Proc. Natl. Acad. Sci. USA* **84,** 8682-8686.

Gordon, D., Merrick, D., Wollner, D. A., and Catterall, W. A. (1988) *Biochemistry* **27,** 7032-7040.

Greenblatt, R. E., Blatt, Y., and Montal, M. (1985) *FEBS Lett.* **193,** 125-134.

Grishin, E. V., Kovalenko, V. A., Pashkov, V. N., and Shamotienko, O. G. (1984) *Biologicheskie Membrany* **8,** 858-867.

Guy, H. R. and Seetharamulu, P. (1986) *Proc. Natl. Acad. Sci. USA* **83,** 508-512.

Guy, H.R. *Molecular Biology of Ion Channels: Current Topics in Membrane Transport.* W. Agnew, Ed, (Academic Press, New York), in press.

Hamill, O.P., Marty, A., Neher, E., Sackmann, B., and Sigworth, F.J. (1981) *Pfluegers Arch.* **391,** 85.

Hartshorne, R.P. and Catterall, W.A. (1984) *J. Biol. Chem.* **259,** 1667-1675.

Hartshorne, R.P., Keller, B.U., Talvenheimo, J.A., Catterall, W.A., and Montal, M. (1985) *Proc. Natl. Acad. Sci. USA* **82,** 240-244.

Hartshorne, R.P., Messner, D.J., Coppersmith, J.C., and Catterall, W.A. (1982) *J. Biol. Chem.* **257,** 13888-13891.

Hille, B. (1984) *Ionic Channels in Excitable Membranes*, Sinauer Associates Inc., Sunderland, MA.

Jover, E., Massacrier, A., Cau, P., Martin, M.-F., and Couraud, F. (1988) *J. Biol. Chem.* **263,** 1542-1548.

Kayano, T., Noda, M., Flockerzi, V., Takahashi, H., and Numa, S. (1988) *FEBS Lett.* **228,** 187-194.

Kyte, J. and Rodriguez, H. (1983) *Anal. Biochem.* **133,** 515-522.

Maizel, J.V. (1971) *Meth. Virol.* **51,** 179-224.

Meiri, H., et al., (1987) *Proc. Natl. Acad. Sci. U.S.A.* **84,** 5058 .

Merrick, D. and Catterall, W.A., unpublished results.

Messner, D. J. and Catterall, W. A. (1985) *J. Biol. Chem.* **260,** 10597-10604.

Messner, D. J., Feller, D. J., Scheuer, T., and Catterall, W. A. (1986) *J. Biol. Chem.* **261,** 14882-14890.

Meves, H., Simard, J. M., and Watt, D. D. (1986) *Ann. NY Acad. Sci.* **479,** 113-132.

Noda, M., et al. (1984) *Nature* **312,** 121.

Noda, M., et al. (1986a) *Nature* **320,** 188-192.

Noda, M., et al. (1986b) *Nature* **322,** 826.

Oxford, G.S., Wu, C.M., and Narahashi, T. (1978) *J. Gen. Physiol.* **71,** 227.

Patlak, J. and Horn, R. (1982) *J. Gen. Physiol.* **79,** 333.

Poli, M.A., Mende, T. J., and Baden, D. G. (1986) *Mol. Pharmacol.* **30,** 129-135.

Ray, R., Morrow, C. S., and Catterall W. A. (1978) *J. Biol. Chem.* **253,** 7307-7313.

Ritchie, J.M. and Rogart, R. B. (1977) *Rev. Physiol. Biochem. Pharmacol.* **79,** 1-49.

Rochat, H., Bernard, P., and Couraud, F. (1979) *Advances in Cytopharmacol.* **3,** 325-334.

Rojas, E. and Rudy, B. (1976) *J. Gen. Physiol.* **262,** 501.

Rossie, S., Gordon, D., and Catterall, W. A. (1987) *J. Biol. Chem.* **262,** 17530-17535.

Ruppersberg, J.P., Schurz, A., and Ruedel, R. (1987) *Neurosci. Lett.* **78,** 166.

Salgado, V.L., Yeh, J.Z., and Narahashi, T. (1985) *Biophys. J.* **47,** 567.

Schmidt, J. W. and Catterall, W. A. (1987) *J. Biol. Chem.*, **262,** 13713-13723.

Sharkey, R. G., Beneski, D. A., and Catterall, W. A. (1984) *Biochemistry* **23,** 6078-6086.

Strichartz, G., Rando, T., and Wang, G. K. (1987) *Ann. Rev. Neurosci.* **10,** 237-267.

Talvenheimo, J.A., Tamkun, M.M., and Catterall, W.A. (1982) *J. Biol. Chem.* **257**, 11868-11871.

Tamkun, M.M. and Catterall, W.A. (1981) *Mol. Pharmacol.* **19**, 78-86.

Tamkun, M.M., Talvenheimo, J.A., and Catterall, W.A. (1984) *J. Biol. Chem.* **259**, 1688.

Tejedor, F.J. and Catterall, W.A. (1988) *Biochemistry*, in press.

Tejedor, F.J. and Catterall, W.A. (1988) *Proc. Natl. Acad. Sci. USA*, in press.

Vandenberg C.A. and Horn, R. (1984) *J. Gen. Physiol.* **84**, 535.

Weiss, R.E. and Horn, R. (1986) *Science* **233**, 361.

Wollner D.A. and Catterall, W.A. (1986) *Proc. Natl. Acad. Sci. U.S.A.* **83**, 8424.

DISTRIBUTION LIST

5 copies	Commander U.S. Army Medical Research Institute of Infectious Diseases ATTN: SGRD-UIZ-M Fort Detrick, Frederick, MD 21701-5011
1 copy	Commander U.S. Army Medical Research and Development Center ATTN: SGRD-RMI-S Fort Detrick, Frederick, MD 21701-5012
12 copies	Defense Technical Information Center (DTIC) ATTN: DTIC-DDAC Cameron Station Alexandria, VA 22304-6145
1 copy	Dean School of Medicine Uniformed Services University of the Health Sciences 4301 Jones Bridge Road Bethesda, MD 20814-4799
1 copy	Commandant Academy of Health Sciences, U.S. Army ATTN: AHS-CDM Fort Sam Houston, TX 78234-6100